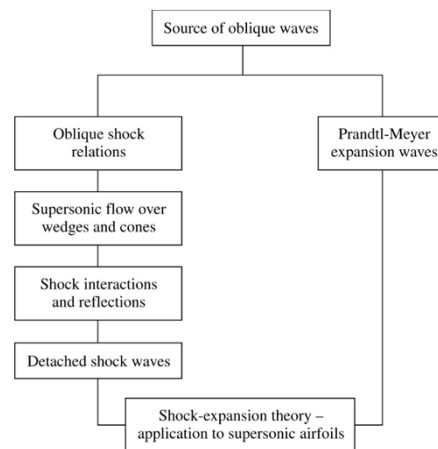


Ch9 Oblique Shock Wave

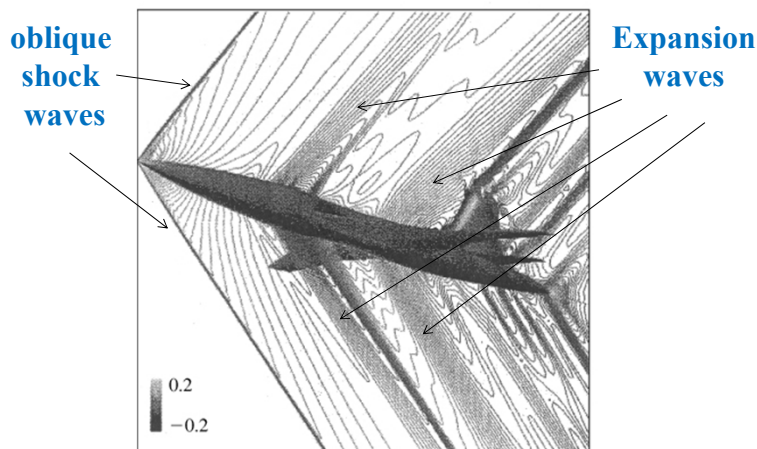
Chapter 9

OBlique SHOCK AND EXPANSION WAVES 503

- 9.1 Introduction 503
- 9.2 Oblique Shock Relations 508
- 9.3 Supersonic Flow Over Wedges and Cones 521
- 9.4 Shock Interactions and Reflections 525
- 9.5 Detached Shock Wave in Front of a Blunt Body 530
- 9.6 Prandtl-Meyer Expansion Waves 532
- 9.7 Shock-Expansion Theory: Applications to Supersonic Airfoils 544
- 9.8 A Comment on Lift and Drag Coefficients 548
- 9.9 Historical Note: Ernst Mach—A Biographical Sketch 548

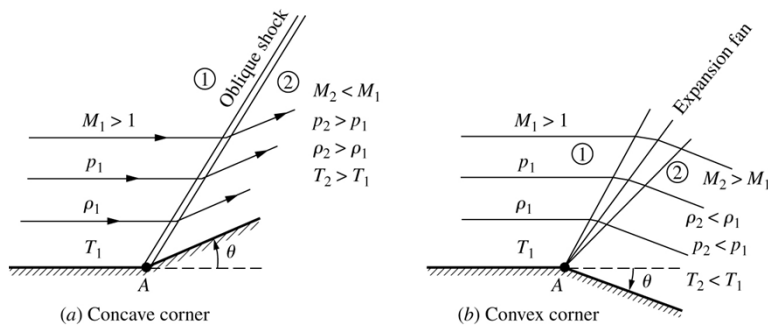


Introduction



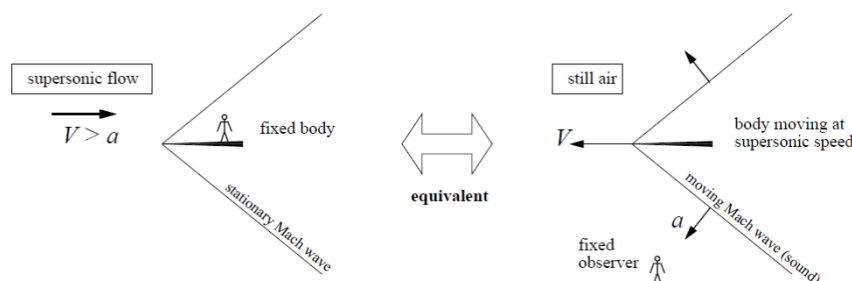
$M=1.7$

Supersonic flow over a corner



Mach Waves

Small disturbances created by a slender body ($\theta \ll 1$) in a supersonic flow will propagate diagonally away as Mach waves. These consist of small **isentropic** variations in ρ , V , p , and h , and are loosely analogous to the water waves sent out by a speed boat. Mach waves appear stationary with respect to the object generating them, but when viewed relative to the still air, they are in fact indistinguishable from sound waves, and **their normal-direction speed of propagation is equal to a , the speed of sound**. Mach waves can be either **compression waves ($p_2 > p_1$)** or **expansion waves ($p_2 < p_1$)**, but in either case their strength is by definition very small ($|p_2 - p_1| \ll p_1$).



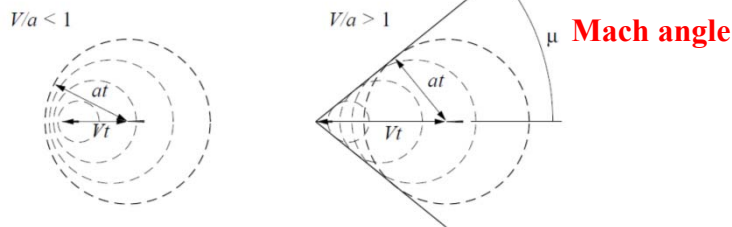
Reading: Anderson 9.1

The Mach angle (μ) of a Mach wave

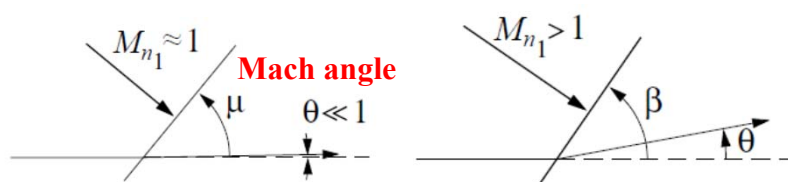
The angle μ of a Mach wave relative to the flow direction is called the **Mach angle**. It can be determined by considering the wave to be the superposition of many pulses emitted by the body, each one producing a disturbance circle (in 2-D) or sphere (in 3-D) which expands at the speed of sound a . At some time interval t after the pulse is emitted, the radius of the circle will be at , while the body will travel a distance Vt . The Mach angle is then seen to be

$$\mu = \arcsin \frac{at}{Vt} = \arcsin \frac{1}{M}$$

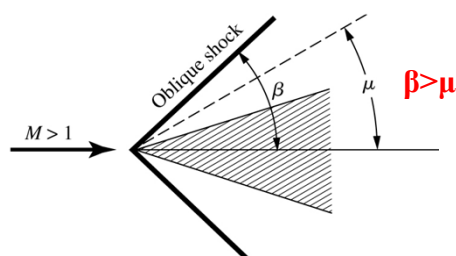
which can be defined at any point in the flow. In the subsonic flow case where $M = V/a < 1$ the expanding circles do not coalesce into a wave front, and the Mach angle is not defined.



Mach Wave v.s. Oblique Shock Wave



small disturbances **finite disturbances**

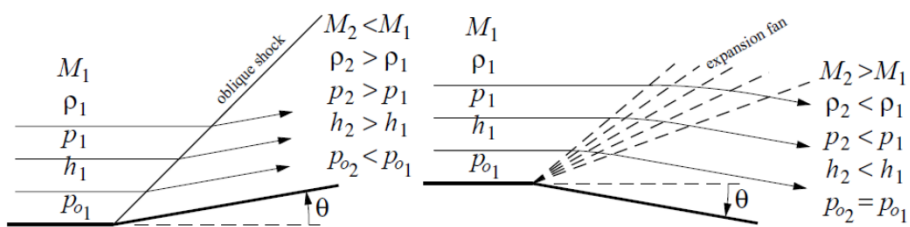


Oblique Shock and Expansion Waves

A body of **finite thickness**, however, will generate oblique waves of finite strength, and now we must distinguish between compression and expansion types. The simplest body shape for generating such waves is

- a **concave** corner, which generates an **oblique shock** (compression), or
- a **convex** corner, which generates an **expansion fan**

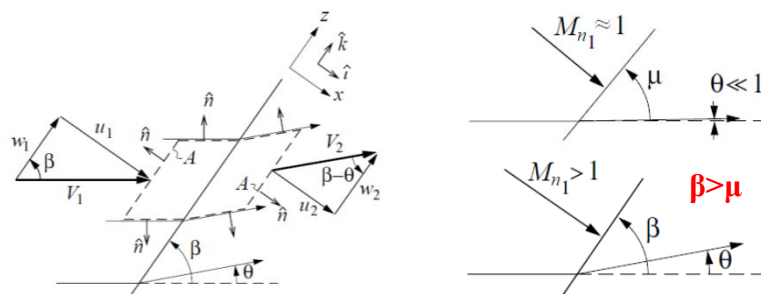
The flow quantity changes across an oblique shock are in the same direction as across a normal shock, and across an expansion fan they are in the opposite direction. **One important difference is that p_0 decreases across the shock (non-isentropic), while the fan is isentropic, so that it has no loss of total pressure across the expansion fans, and hence $p_{02} = p_{01}$.**



Oblique Shock Wave geometry and analysis

As with the normal shock case, a control volume analysis is applied to the oblique shock flow, using the **control volume** shown in the figure. The top and bottom boundaries are chosen to lie along streamlines so that only the boundaries parallel to the shock, with area A, have mass flow across them. **Velocity components are taken in the x-z coordinates normal and tangential to the shock**, as shown. The tangential z axis is tilted from the upstream flow direction by the wave angle β , which is the same as the Mach angle μ only if the shock is extremely weak. **For a finite-strength shock, $\beta > \mu$** . The upstream flow velocity components are

$$u_1 = V_1 \sin \beta \quad w_1 = V_1 \cos \beta$$



1D Flow across Oblique Shock Wave

Mass continuity

$$\begin{aligned} \iint \rho \vec{V} \cdot \hat{n} dA &= 0 \\ -\rho_1 u_1 A + \rho_2 u_2 A &= 0 \\ \boxed{\rho_1 u_1 = \rho_2 u_2} \end{aligned} \quad (1)$$

x-Momentum

$$\begin{aligned} \iint \rho \vec{V} \cdot \hat{n} u dA + \iint p \hat{n} \cdot \hat{i} dA &= 0 \\ -\rho_1 u_1^2 A + \rho_2 u_2^2 A - p_1 A + p_2 A &= 0 \\ \boxed{\rho_1 u_1^2 + p_1 = \rho_2 u_2^2 + p_2} \end{aligned} \quad (2)$$

z-Momentum

$$\begin{aligned} \iint \rho \vec{V} \cdot \hat{n} w dA + \iint p \hat{n} \cdot \hat{k} dA &= 0 \\ -\rho_1 u_1 A w_1 + \rho_2 u_2 A w_2 &= 0 \\ \boxed{w_1 = w_2} \end{aligned} \quad (3)$$

Energy

$$\begin{aligned} \iint \rho \vec{V} \cdot \hat{n} h_o dA &= 0 \\ -\rho_1 u_1 h_{o1} A + \rho_2 u_2 h_{o2} A &= 0 \\ \boxed{h_{o1} = h_{o2}} \\ h_1 + \frac{1}{2} (u_1^2 + w_1^2) &= h_2 + \frac{1}{2} (u_2^2 + w_2^2) \\ \boxed{h_1 + \frac{1}{2} u_1^2 = h_2 + \frac{1}{2} u_2^2} \end{aligned} \quad (4)$$

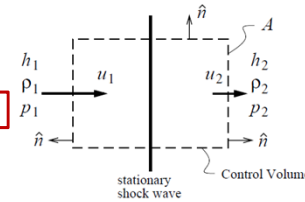
Equation of State

$$\boxed{p_2 = \frac{\gamma-1}{\gamma} \rho_2 h_2} \quad (5)$$

1D Flow across Normal Shock Wave

Mass continuity

$$\begin{aligned} \iint \rho \vec{V} \cdot \hat{n} dA &= 0 \\ -\rho_1 u_1 A + \rho_2 u_2 A &= 0 \\ \boxed{\rho_1 u_1 = \rho_2 u_2} \quad (1) \end{aligned}$$



x-Momentum

$$\begin{aligned} \iint \rho \vec{V} \cdot \hat{n} u dA + \iint p \hat{n} \cdot \hat{i} dA &= 0 \\ -\rho_1 u_1^2 A + \rho_2 u_2^2 A - p_1 A + p_2 A &= 0 \\ \boxed{\rho_1 u_1^2 + p_1 = \rho_2 u_2^2 + p_2} \end{aligned} \quad (2)$$

Energy

$$\begin{aligned} \iint \rho \vec{V} \cdot \hat{n} h_o dA &= 0 \\ -\rho_1 u_1 h_{o1} A + \rho_2 u_2 h_{o2} A &= 0 \\ \boxed{h_{o1} = h_{o2}} \\ h_1 + \frac{1}{2} u_1^2 &= h_2 + \frac{1}{2} u_2^2 \end{aligned} \quad (3)$$

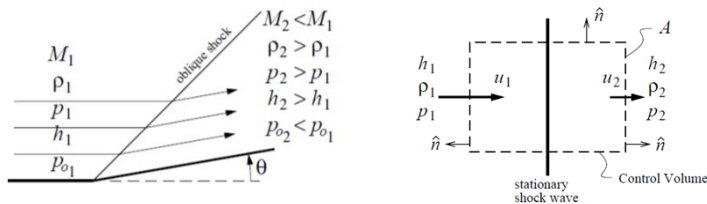
Equation of State

$$\boxed{p_2 = \frac{\gamma-1}{\gamma} \rho_2 h_2 \quad or \quad p_2 = \rho_2 R T_2} \quad (4)$$

Oblique/Normal Shock Equivalence

It is apparent that equations for oblique shock are in fact identical to the normal-shock equations derived earlier. **The one addition z-momentum equation (3) simply states that the tangential velocity component doesn't change across a shock.**

This can be physically interpreted if we examine the oblique shock from the viewpoint of an observer moving with the everywhere-**constant tangential velocity $w = w_1 = w_2$** . As shown in the figure, the moving observer sees a normal shock with velocities u_1 , and u_2 . The static fluid properties p , ρ , h , a are of course the same in both frames.



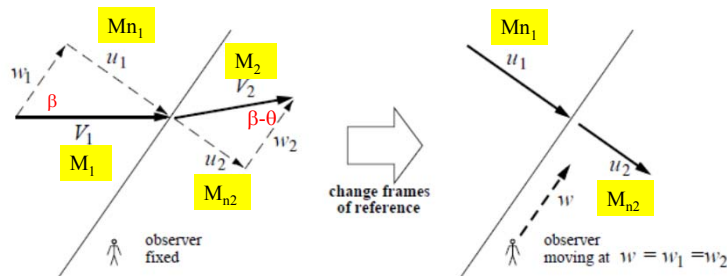
Oblique Shock Relations

The effective equivalence between an oblique and a normal shock allows reuse of the already derived normal shock jump relations. We only need to construct the necessary transformation from one frame to the other.

First we define the normal Mach number components seen by the moving observer.

$$M_{n1} \equiv \frac{u_1}{a_1} = \frac{V_1 \sin \beta}{a_1} = M_1 \sin \beta \quad (6)$$

$$M_{n2} \equiv \frac{u_2}{a_2} = \frac{V_2 \sin(\beta - \theta)}{a_2} = M_2 \sin(\beta - \theta)$$



These are then related via our previous normal-shock $M_2 = f(M_1)$ relation, if we make the substitutions $M_1 \rightarrow M_{n1}$, $M_2 \rightarrow M_{n2}$. The fixed-frame M_2 then follows from geometry.

$$M_{n2}^2 = \frac{1 + \frac{\gamma-1}{2} M_{n1}^2}{\gamma M_{n1}^2 - \frac{\gamma-1}{2}} \quad (7) \quad M_2 = \frac{M_{n2}}{\sin(\beta - \theta)} \quad (8)$$

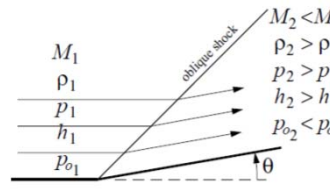
The static property ratios are likewise obtained using the previous normal-shock relations.

$$\frac{\rho_2}{\rho_1} = \frac{(\gamma+1)M_{n1}^2}{2 + (\gamma-1)M_{n1}^2} \quad (9)$$

$$\frac{p_2}{p_1} = 1 + \frac{2\gamma}{\gamma+1} (M_{n1}^2 - 1) \quad (10)$$

$$\frac{h_2}{h_1} = \frac{p_2 \rho_1}{p_1 \rho_2} \quad (11)$$

$$\frac{p_{o2}}{p_{o1}} = \frac{p_2}{p_1} \left(\frac{h_1}{h_2} \right)^{\gamma/(\gamma-1)} \quad (12)$$



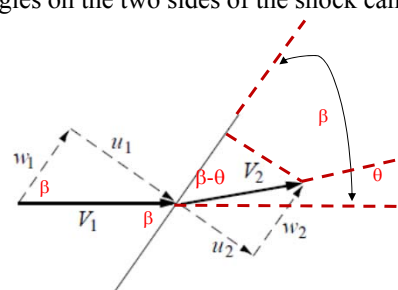
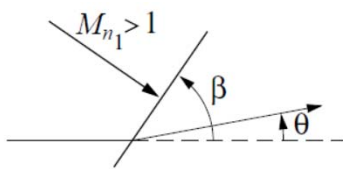
$$\frac{\rho_2}{\rho_1} = (1 + \frac{\gamma-1}{2} M_1^2)^{-\frac{1}{\gamma}}$$

$$\frac{p_2}{p_1} = (1 + \frac{\gamma-1}{2} M_1^2)^{-\frac{2}{\gamma}}$$

$$\frac{T_2}{T_1} = (1 + \frac{\gamma-1}{2} M_1^2)^{-1}$$

$$\frac{p_{o2}}{p_{o1}} = \frac{p_2}{p_1} \frac{p_1}{p_{o1}} = \frac{p_2}{p_1} \left(\frac{T_{02}}{T_1} \right)^{\frac{\gamma}{\gamma-1}} \left(\frac{T_1}{T_{01}} \right)^{\frac{\gamma}{\gamma-1}} = \frac{p_2}{p_1} \left(\frac{T_1}{T_2} \right)^{\frac{\gamma}{\gamma-1}} = \frac{p_2}{p_1} \left(\frac{h_1}{h_2} \right)^{\frac{\gamma}{\gamma-1}}$$

To allow application of the above relations, we still require the wave angle β . Using the result $w_1 = w_2$, the velocity triangles on the two sides of the shock can be related by



$$\tan(\beta - \theta) = \frac{u_2}{w_2}$$

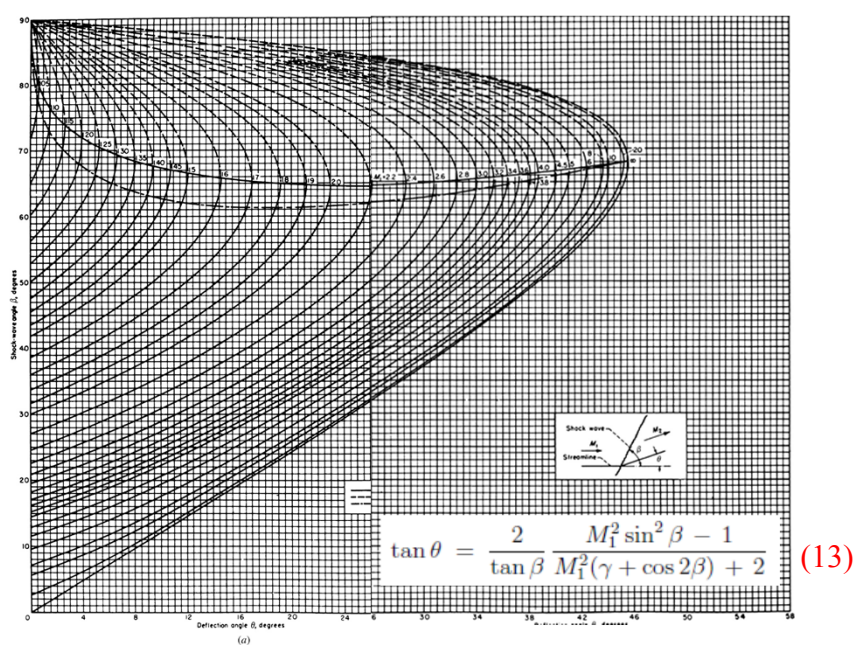
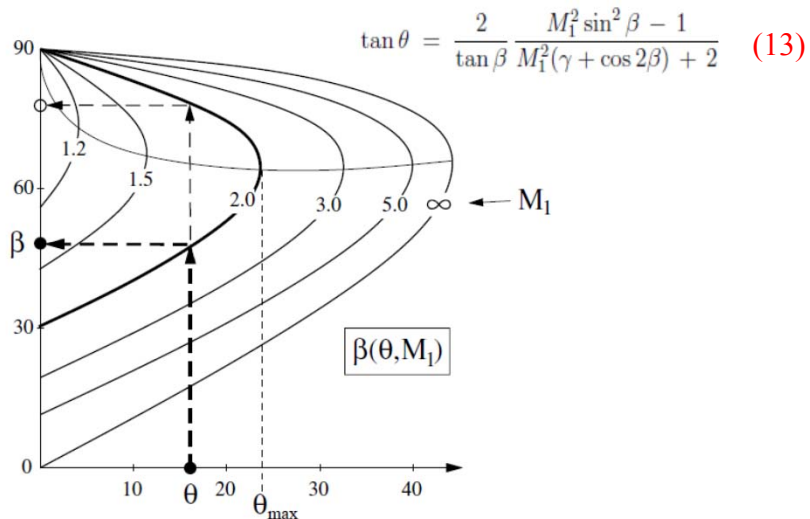
$$\tan \beta = \frac{u_1}{w_1}$$

$$\frac{\tan(\beta - \theta)}{\tan \beta} = \frac{u_2 / w_1}{u_1 / w_1} = \frac{u_2}{u_1} = \frac{\rho_1}{\rho_2} = \frac{(\gamma+1)M_{n1}^2}{2+(\gamma-1)M_{n1}^2} = \frac{(\gamma+1)M_1^2 \sin^2 \beta}{2+(\gamma-1)M_1^2 \sin^2 \beta}$$

$$\text{Solving this for } \theta \text{ gives } \tan \theta = \frac{2}{\tan \beta} \frac{M_1^2 \sin^2 \beta - 1}{M_1^2 (\gamma + \cos 2\beta) + 2} \quad (13)$$

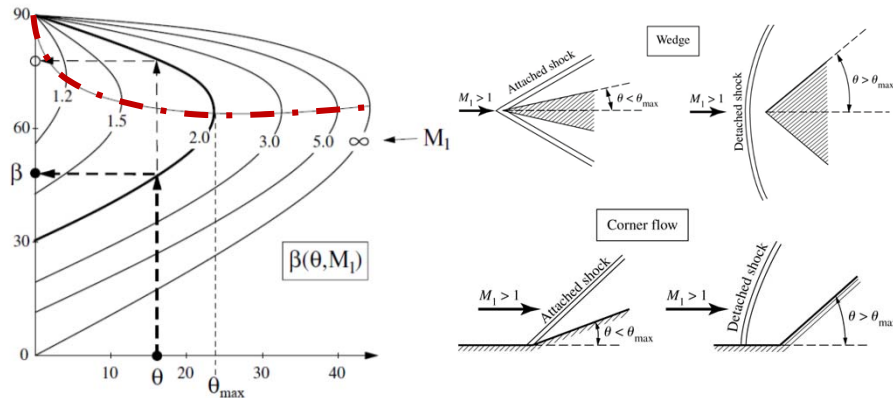
which is an implicit definition of the function $\beta(\theta, M_1)$.

Use of equation (13) in the first step can be problematic, since it must be numerically solved to obtain the $\beta(\theta, M_1)$ result. A convenient alternative is to obtain this result graphically, from an oblique shock chart, illustrated in the figure below.

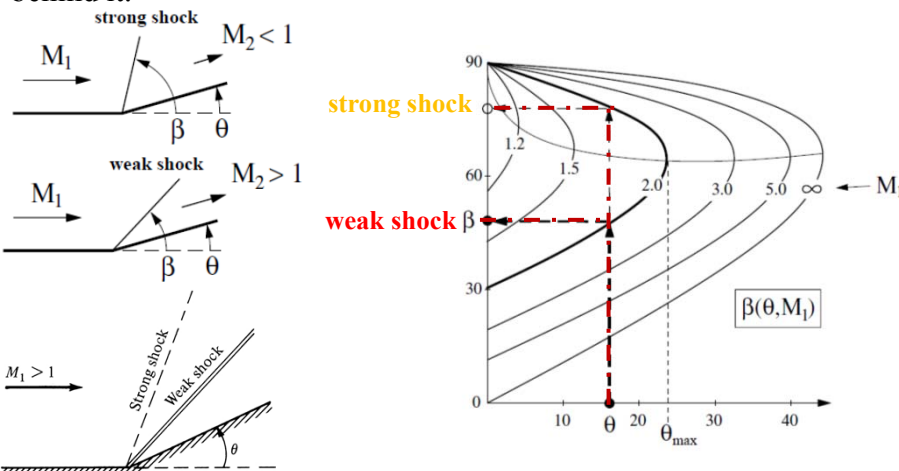


The chart also reveals a number of important features:

- (1) There is a maximum turning angle θ_{\max} for any given upstream Mach number M_1 . If the wall angle exceeds this, or $\theta > \theta_{\max}$, **no oblique shock is possible. Instead, a detached shock forms ahead of the concave corner.** Such a detached shock is in fact the same as a bow shock discussed earlier.

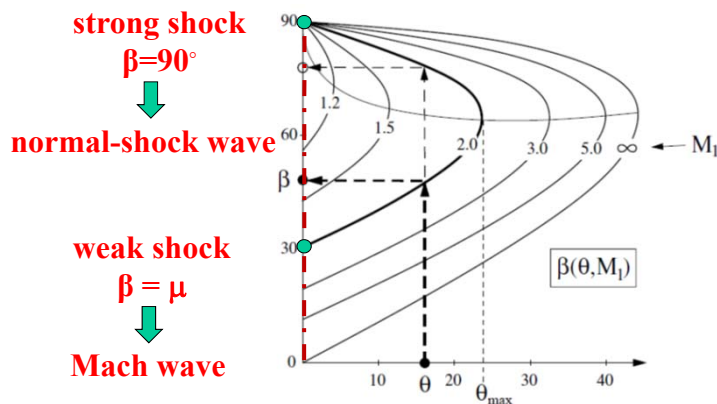


- (2) If $\theta < \theta_{\max}$, **two distinct oblique shocks with two different β angles are physically possible.** The smaller β case is called a **weak shock**, and is the one most likely to occur in a typical supersonic flow. The larger β case is called a **strong shock**, and is unlikely to form over a straight-wall wedge. The strong shock has a subsonic flow behind it.

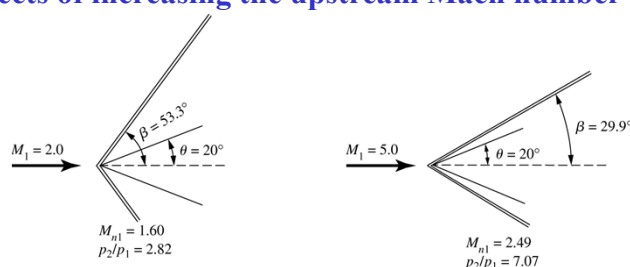


(3) If $\theta = 0$, then β equals either 90° or μ .

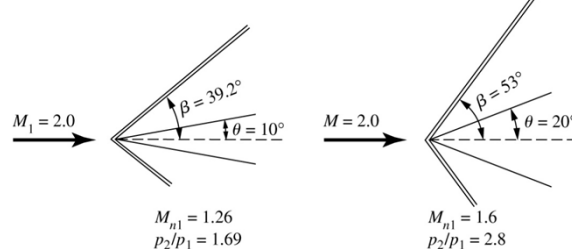
- The case of $\beta = 90^\circ$ corresponds to a **normal shock wave** (i.e. the normal shocks discussed in Chap. 8 belong to the family of strong shock solutions).
- The case of $\beta = \mu$ corresponds to the **Mach wave**. In both cases, the flow streamlines experience no deflection across the wave.



(4) Effects of increasing the upstream Mach number



(5) Effect of increasing the deflection angle theta.



Oblique-Shock Analysis: Summary

Starting from the known **upstream Mach number M_1** and the **flow deflection angle (body surface angle) θ** , the oblique-shock analysis proceeds as follows.

$$\tan \theta = \frac{2}{\tan \beta} \frac{M_1^2 \sin^2 \beta - 1}{M_1^2(\gamma + \cos 2\beta) + 2} \quad M_{n_2}^2 = \frac{1 + \frac{\gamma-1}{2} M_{n_1}^2}{\gamma M_{n_1}^2 - \frac{\gamma-1}{2}} \quad M_2 = \frac{M_{n_2}}{\sin(\beta - \theta)}$$

$\theta, M_1 \xrightarrow{\text{Eq.(13)}} \beta \xrightarrow{\text{Eq.(6)}} M_{n_1} \xrightarrow{\text{Eq.s.}(\gamma)-\text{Eq.(12)}} M_{n_2}, M_2, \frac{p_2}{\rho_1}, \frac{p_2}{p_1}, \frac{h_2}{h_1}, \frac{p_{o_2}}{p_{o_1}}$

$M_{n_1} = M_1 \sin \beta$

$\frac{p_2}{\rho_1} = \frac{(\gamma+1)M_{n_1}^2}{2 + (\gamma-1)M_{n_1}^2}$

$\frac{p_2}{p_1} = 1 + \frac{2\gamma}{\gamma+1} (M_{n_1}^2 - 1)$

$\frac{h_2}{h_1} = \frac{p_2 \rho_1}{p_1 \rho_2}$

$\frac{p_{o_2}}{p_{o_1}} = \frac{p_2}{p_1} \left(\frac{h_1}{h_2} \right)^{\gamma/(\gamma-1)}$

The diagram illustrates an oblique shock wave (labeled 'oblique shock') impacting a body surface at an angle θ . The upstream conditions are labeled $M_1, \rho_1, p_1, h_1, p_{o_1}$. The downstream conditions are labeled $M_2 < M_1, \rho_2 > \rho_1, p_2 > p_1, h_2 > h_1, p_{o_2} < p_{o_1}$. The deflection angle is β .

Example 9.1. Consider a supersonic flow with $M = 2$, $p = 1 \text{ atm}$, and $T = 288 \text{ K}$. This flow is deflected at a compression corner through 20° . Calculate M , p , T , p_0 , and T_0 behind the resulting oblique shock wave.

Solution. From Fig. 9.7, for $M_1 = 2$ and $\theta = 20^\circ$, $\beta = 53.4^\circ$. Hence, $M_{n,1} = M_1 \sin \beta = 2 \sin 53.4^\circ = 1.606$. From App. B, for $M_{n,1} = 1.60$ (rounded to the nearest table entry),

$$M_{n,2} = 0.6684 \quad \frac{p_2}{p_1} = 2.82 \quad \frac{T_2}{T_1} = 1.388 \quad \frac{p_{o,2}}{p_{o,1}} = 0.8952$$

Hence,

$$M_2 = \frac{M_{n,2}}{\sin(\beta - \theta)} = \frac{0.6684}{\sin(53.4 - 20)} = [1.21]$$

Note: For oblique shocks, the entry for $P_{o'}/P_1$ in App. B cannot be used to obtain $P_{o,2}$; this entry in App. B is for normal shocks only.

$$p_2 = \frac{p_2}{p_1} p_1 = 2.82(1 \text{ atm}) = [2.82 \text{ atm}]$$

$$T_2 = \frac{T_2}{T_1} T_1 = 1.388(288) = [399.7 \text{ K}]$$

$$\frac{p_{o,2}}{p_2} = (1 + \frac{\gamma-1}{2} M_2^2)^{\frac{\gamma}{\gamma-1}}$$

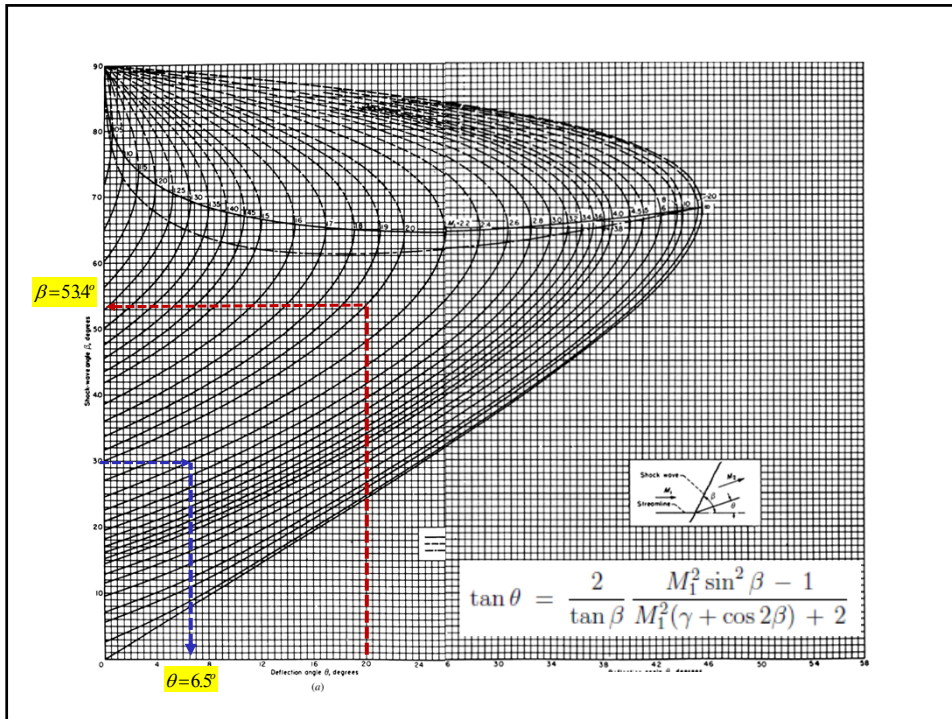
$$\frac{p_{o,2}}{p_2} = (1 + \frac{0.4}{2} 1.2^2)^{\frac{1.4}{0.4}} = 2.45$$

For $M_1 = 2$, from App. A, $p_{o,1}/p_1 = 7.824$ and $T_{o,1}/T_1 = 1.8$; thus,

$$\frac{p_{o,2}}{p_{o,1}} \frac{p_{o,1}}{p_1} p_1 = 0.8952(7.824)(1 \text{ atm}) = [7.00 \text{ atm}] \quad p_{o,2} = 6909 \text{ atm}$$

The total temperature is constant across the shock. Hence,

$$T_{o,2} = T_{o,1} = \frac{T_{o,1}}{T_1} T_1 = 1.8(288) = [518.4 \text{ K}]$$



Example 9.2. Consider an oblique shock wave with a wave angle of 30° . The upstream flow Mach number is 2.4. Calculate the deflection angle of the flow, the pressure and temperature ratios across the shock wave, and the Mach number behind the wave.

$$\tan \theta = \frac{2}{\tan \beta} \frac{M_1^2 \sin^2 \beta - 1}{M_1^2(\gamma + \cos 2\beta) + 2} \quad (13)$$

Solution. From Fig. 9.7, for $M_1 = 2.4$ and $\beta = 30^\circ$, we have $\theta = 6.5^\circ$. Also,

$$M_{n,1} = M_1 \sin \beta = 2.4 \sin 30^\circ = 1.2$$

From App. B,

$$\frac{p_2}{p_1} = 1.513$$

$$\frac{T_2}{T_1} = 1.128$$

$$M_{n,2} = 0.8422$$

Thus,

$$M_2 = \frac{M_{n,2}}{\sin(\beta - \theta)} = \frac{0.8422}{\sin(30 - 6.5)} = 2.11$$

Example 9.4. Consider a Mach 3 flow. It is desired to slow this flow to a subsonic speed. Consider two separate ways of achieving this: (1) the Mach 3 flow is slowed by passing directly through a normal shock wave; (2) the Mach 3 flow first passes through an oblique shock with a 40° wave angle, and then subsequently through a normal shock. These two cases are sketched in Fig. 9.12. Calculate the ratio of the final total pressure values for the two cases, i.e., the total pressure behind the normal shock for case 2 divided by the total pressure behind the normal shock for case 1. Comment on the significance of the result.

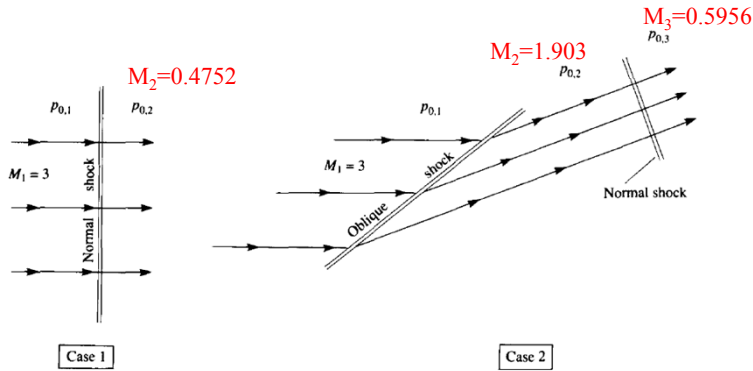


FIGURE 9.12
Illustration for Example 9.4.

Solution. For case 1, at $M = 3$, we have, from App. B,

$$\left(\frac{p_0}{p_{01}}\right)_{\text{case 1}} = 0.3283$$

For case 2, we have $M_{n,1} = M_1 \sin \beta = 3 \sin 40^\circ = 1.93$. From App. B,

$$\frac{p_{02}}{p_{01}} = 0.7535 \quad \text{and} \quad M_{n,2} = 0.588$$

From Fig. 9.7, for $M_1 = 3$ and $\beta = 40^\circ$, we have the deflection angle $\theta = 22^\circ$. Hence,

$$M_2 = \frac{M_{n,2}}{\sin(\beta - \theta)} = \frac{0.588}{\sin(40 - 22)} = 1.90$$

From App. B, for a normal shock with an upstream Mach number of 1.9, we have $p_{03}/p_{02} = 0.7674$. Thus, for case 2,

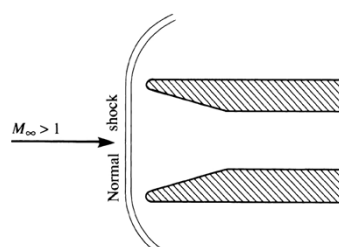
$$\left(\frac{p_{03}}{p_{01}}\right)_{\text{case 2}} = \left(\frac{p_{02}}{p_{01}}\right) \left(\frac{p_{03}}{p_{02}}\right) = (0.7535)(0.7674) = 0.578$$

Hence,

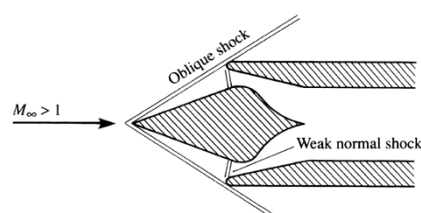
$$\left(\frac{p_{03}}{p_{01}}\right)_{\text{case 2}} / \left(\frac{p_{02}}{p_{01}}\right)_{\text{case 1}} = \frac{0.578}{0.3283} = \boxed{1.76}$$

- Example 9.4 shows that the final total pressure is 76 percent higher for the case of the **multiple shock system (case 2)** in comparison to the single normal shock (case 1).
- In principle, the total pressure is an indicator of **how much useful work can be done by the gas**. The higher the total pressure, the more useful is the flow. Indeed, **losses of total pressure are an index of the efficiency of a fluid flow** - the lower the total pressure loss, the more efficient is the flow process.
- In this example, case 2 is more efficient in slowing the flow to subsonic speeds than case 1 because **the loss in total pressure across the multiple shock system of case 2 is actually less than that for case 1 with a single, strong, normal shock wave**.
- The physical reason for this is straightforward. The loss in total pressure across a normal shock wave becomes particularly severe as the upstream Mach number increases.

If the Mach number of a flow can be reduced *before* passing through a normal shock, the loss in total pressure is much less because the normal shock is weaker. This is the function of the oblique shock, namely, to reduce the Mach number of the flow before passing through the normal shock. Although there is a total pressure loss across the oblique shock also, it is much less than across a normal shock wave at the same upstream Mach number.

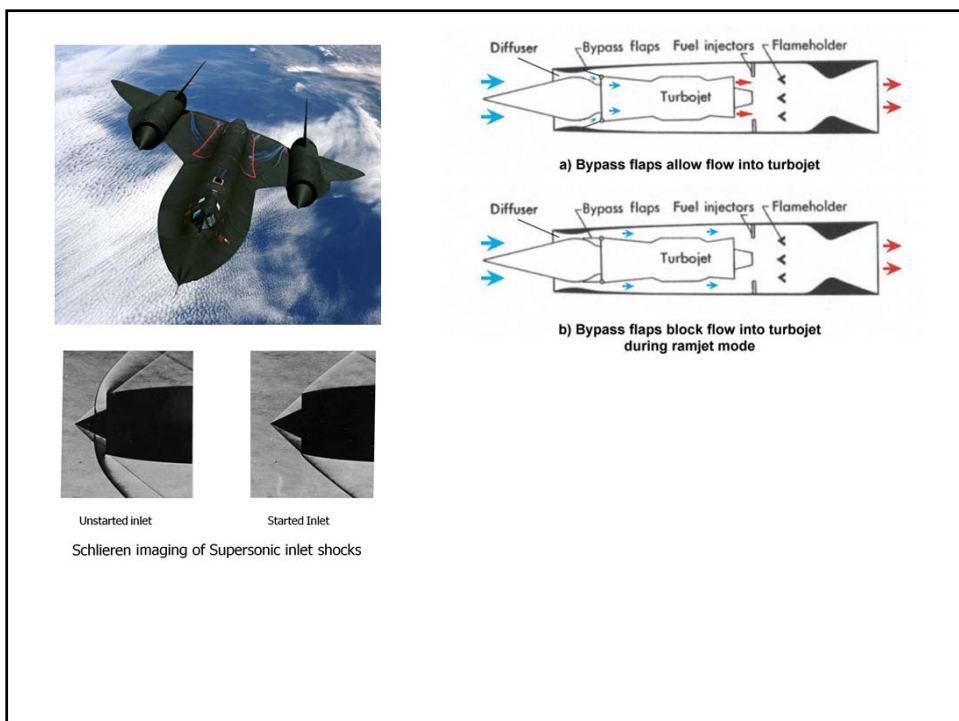
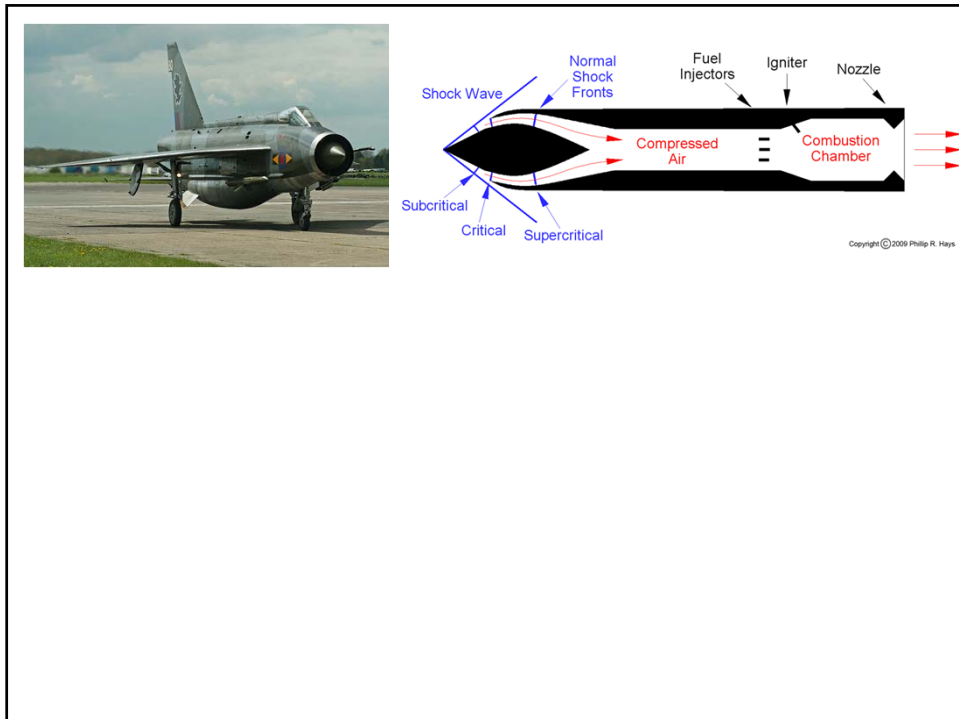


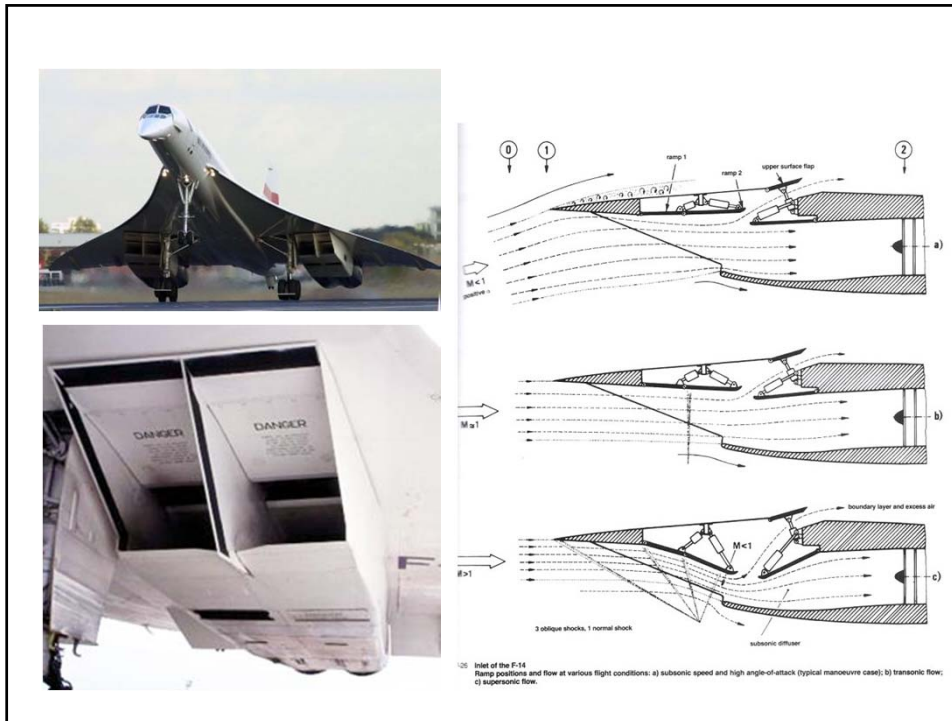
(a) Normal shock inlet



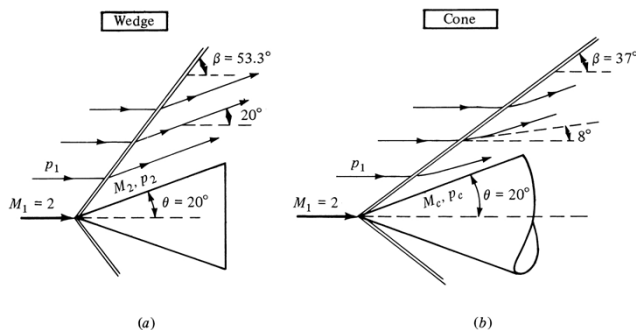
(b) Oblique shock inlet







Supersonic Flow over Wedges and Cones



In comparing the wedge and cone, both with the same 20° angle, the flow over the cone has an extra dimension in which to move, and hence it more easily adjusts to the presence of the conical body in comparison to the two-dimensional wedge. **One consequence of this three-dimensional relieving effect is that the shock wave on the cone is weaker than on the wedge; i.e., it has a smaller wave angle**, as compared in Fig. Specifically, the wave angles for the wedge and cone are 53.3 and 37° , respectively, for the same body angle of 20° and the same upstream Mach number of 2.0 . In the case of the wedge (Fig. a), the streamlines are deflected by exactly 20° through the shock wave, and hence downstream of the shock the flow is exactly parallel to the wedge surface. In contrast, because of the weaker shock on the cone, the streamlines are deflected by only 8° through the shock, as shown in Fig. b. Therefore, between the shock wave and the cone surface, the streamlines must gradually curve upward in order to accommodate the 20° cone.

Example 9.5. Consider a wedge with a 15° half angle in a Mach 5 flow, as sketched in Fig. 9.15. Calculate the drag coefficient for this wedge. (Assume that the pressure over the base is equal to freestream static pressure, as shown in Fig. 9.15.)

Solution. Consider the drag on a unit span of the wedge, D' . Hence,

$$c_d = \frac{D'}{q_1 S} = \frac{D'}{q_1 c(1)} = \frac{D'}{q_1 c}$$

$$D' = 2p_2 l \sin \theta - 2p_1 l \sin \theta = (2l \sin \theta)(p_2 - p_1)$$

$$l = \frac{c}{\cos \theta} \quad D' = (2c \tan \theta)(p_2 - p_1)$$

$$c_d = (2 \tan \theta) \left(\frac{p_2 - p_1}{q_1} \right)$$

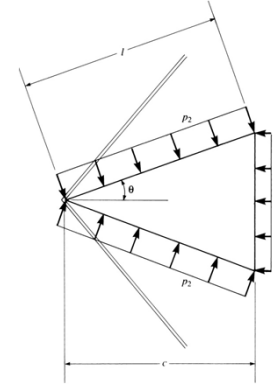
$$q_1 = \frac{1}{2} \rho_1 V_1^2 = \frac{1}{2} \rho_1 \frac{\gamma p_1}{\gamma p_1} V_1^2 = \frac{\gamma p_1}{2 a_1^2} V_1^2 = \frac{\gamma}{2} p_1 M_1^2$$

$$c_d = (2 \tan \theta) \left(\frac{p_2 - p_1}{(\gamma/2)p_1 M_1^2} \right) = \frac{4 \tan \theta}{\gamma M_1^2} \left(\frac{p_2}{p_1} - 1 \right)$$

for $M_1 = 5$ and $\theta = 15^\circ$, $\beta = 24.2^\circ$. Hence, $M_{n,1} = M_1 \sin \beta = 5 \sin (24.2^\circ) = 2.05$

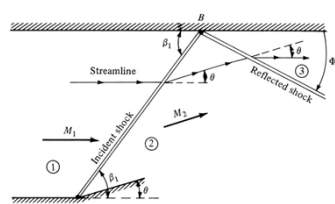
From App. B, for $M_{n,1} = 2.05$, we have $\frac{p_2}{p_1} = 4.736$

$$c_d = \frac{4 \tan \theta}{\gamma M_1^2} \left(\frac{p_2}{p_1} - 1 \right) = \frac{4 \tan 15^\circ}{(1.4)(5)^2} (4.736 - 1) = \boxed{0.114}$$



Shocks are always a drag producing mechanism. The drag in this case is called **wave drag**, and Cd_w is the **wave-drag coefficient**.

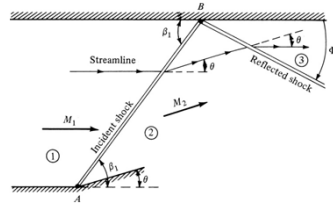
Shock Interactions and Reflections



First, consider an oblique shock wave generated by a concave corner. The deflection angle at the corner is θ , thus generating an **oblique shock at point A** with a **wave angle**, β_1 . Assume that a straight, horizontal wall is present above the corner. The shock wave generated at point A, called the **incident shock wave**, impinges on the upper wall at point B.

Question: Does the shock wave simply disappear at point B? If not, what happens to it? To answer this question, we appeal to our knowledge of shock-wave properties. Examining Fig. we see that the flow in region 2 behind the incident shock is inclined upward at the deflection angle θ . However, the flow must be tangent everywhere along the upper wall; if the flow in region 2 were to continue unchanged, it would run into the wall and have no place to go. Hence, **the flow in region 2 must eventually be bent downward through the angle θ in order to maintain a flow tangent to the upper wall**. Nature accomplishes this downward deflection via a second shock wave originating at the impingement point B. This second shock is called the **reflected shock wave**.

Shock Reflections



The purpose of the reflected shock is to deflect the flow in region 2 so that it is parallel to the upper wall in region 3, thus preserving the wall boundary condition. The strength of the reflected shock wave is weaker than the incident shock. This is because $M_2 < M_1$, and M_2 represents the upstream Mach number for the reflected shock wave.

Since the deflection angles θ are the same, whereas the reflected shock sees a lower upstream Mach number, we know that the reflected wave must be weaker. For this reason, the angle the reflected shock makes with the upper wall, Φ , is not equal to β . The properties of the reflected shock are uniquely defined by M_1 and θ .

Since M_2 is in turn uniquely defined by M_1 and θ , then the properties in region 3 behind the reflected shock as well as the angle Φ are easily determined from the given conditions of M_1 and θ by using the procedure of as follows:

1. Calculate the properties in region 2 from the given M_1 and θ . This gives us M_2
2. Calculate the properties in region 3 from the value of M_2 calculated above and the known deflection angle θ

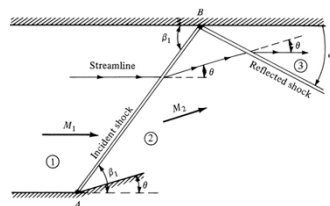
Example 9.6. Consider an oblique shock wave generated by a compression corner with a 10° deflection angle. The Mach number of the flow ahead of the corner is 3.6; the flow pressure and temperature are standard sea level conditions. The oblique shock wave subsequently impinges on a straight wall opposite the compression corner. The geometry for this flow is given in Fig. 9.17. Calculate the angle of the reflected shock wave, Φ , relative to the straight wall. Also, obtain the pressure, temperature, and Mach number behind the reflected wave.

Solution. From the θ - β - M diagram, Fig. 9.7, for $M_1 = 3.6$ and $\theta = 10^\circ$, $\beta_1 = 24^\circ$. Hence,

$$M_{n,1} = M_1 \sin \beta_1 = 3.6 \sin 24^\circ = 1.464$$

From App. B,

$$M_{n,2} = 0.7157, \quad \frac{p_2}{p_1} = 2.32, \quad \text{and} \quad \frac{T_2}{T_1} = 1.294$$



Also,

$$M_2 = \frac{M_{n,2}}{\sin(\beta - \theta)} = \frac{0.7157}{\sin(24 - 10)} = 2.96$$

These are the conditions behind the incident shock wave. They constitute the upstream flow properties for the reflected shock wave. We know that the flow must be deflected again by $\theta = 10^\circ$ in passing through the reflected shock. Thus, from the θ - β - M diagram, for $M_2 = 2.96$ and $\theta = 10^\circ$, we have the wave angle for the reflected shock, $\beta_2 = 27.3^\circ$. Note that β_2 is *not* the angle the reflected shock makes with respect to the upper wall; rather, by definition of the wave angle, β_2 is the angle between the reflected shock and the direction of the flow in region 2. The shock angle relative to the wall is, from the geometry shown in Fig. 9.17,

$$\Phi = \beta_2 - \theta = 27.3 - 10 = 17.3^\circ$$

Also, the normal component of the upstream Mach number relative to the reflected shock is $M_2 \sin \beta_2 = (2.96) \sin 27.3^\circ = 1.358$. From App. B,

$$\frac{p_3}{p_2} = 1.991, \quad \frac{T_3}{T_2} = 1.229, \quad M_{n,3} = 0.7572$$

Hence,

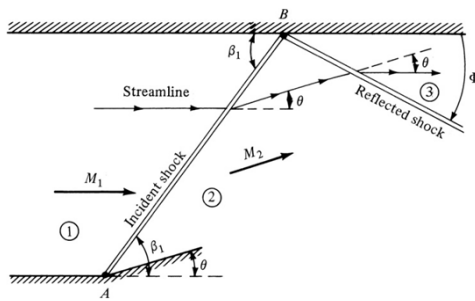
$$M_3 = \frac{M_{n,3}}{\sin(\beta_2 - \theta)} = \frac{0.7572}{\sin(27.3 - 10)} = 2.55$$

For standard sea level conditions, $p_1 = 2116 \text{ lb/ft}^3$ and $T_1 = 519^\circ\text{R}$. Thus,

$$\frac{p_3}{p_2} \frac{p_2}{p_1} p_1 = (1.991)(2.32)(2116) = 9774 \text{ lb/ft}^3$$

$$\frac{T_3}{T_2} \frac{T_2}{T_1} T_1 = (1.229)(1.294)(519) = 825^\circ\text{R}$$

Note that the reflected shock is weaker than the incident shock, as indicated by the smaller pressure ratio for the reflected shock, $p_3/p_2 = 1.991$ as compared to $p_2/p_1 = 2.32$ for the incident shock.



Mach Reflection

An interesting situation can arise as follows. Assume that M_1 is only slightly above the minimum Mach number necessary for a straight, attached shock wave at the given deflection angle θ . However, we know that the Mach number decreases across a shock, i.e., $M_2 < M_1$. This decrease may be enough such that M_2 is *not* above the minimum Mach number for the required deflection θ through the reflected shock. In such a case, the regular reflection as shown in Fig. 9.17 is not possible. Nature handles this situation by creating the wave pattern shown in Fig. 9.18. Here, the originally straight incident shock becomes curved as it nears the upper wall and becomes a **normal shock** wave at the upper wall. This allows the streamline at the wall to continue parallel to the wall behind the shock intersection. In addition, a **curved reflected shock** branches from the normal shock and propagates downstream. This wave pattern, shown in Fig. 9.18, is called a **Mach reflection**.

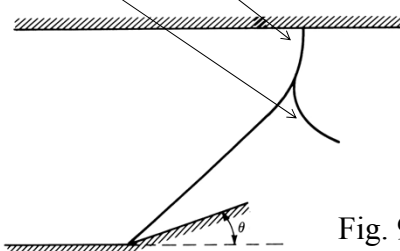
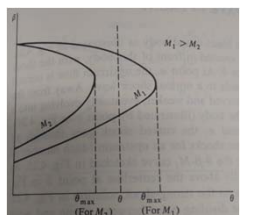
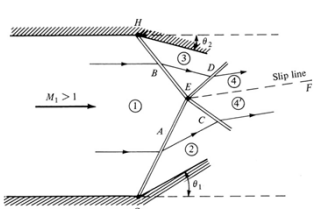


Fig. 9.18

Shock Interactions



A shock wave is generated by the concave corner at point G and propagates upward. Denote this wave as shock A. Another shock wave is generated by the concave corner at point H, and propagates downward. Denote this wave as shock B. The picture shown in Fig. 9.19 is the intersection of right- and left running shock waves. The intersection occurs at point E.

At the intersection, wave A is refracted and continues as wave D. Similarly, wave B is refracted and continues as wave C. The flow behind the refracted shock D is denoted by region 4; the flow behind the refracted shock C is denoted by region 4'. These two regions are divided by a **slip line**, EF. Across the slip line, the pressures are constant, i.e., $P_4 = P_{4'}$, and the direction (but not necessarily the magnitude) of velocity is the same, namely, parallel to the slip line. All other properties in regions 4 and 4' are different, most notably the entropy ($S_4 \neq S_{4'}$). The conditions which must hold across the slip line, along with the known M_1 , θ_1 , and θ_2 , uniquely determine the shock-wave interaction shown in Fig. (See chap. 4 of Ref. 21 for details concerning the calculation of this interaction.)

Shock Interactions

$P_3 = P_5$? $\theta_3 = \theta_5$?
 ↓
 reflected wave (weak shock
or expansion wave)
 ↓
 $P_4 = P_5$ $\theta_4 = \theta_5$

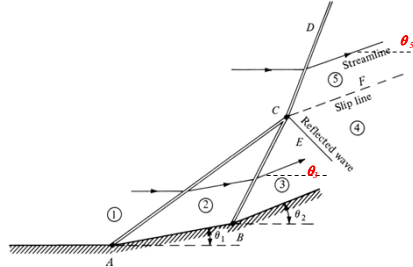
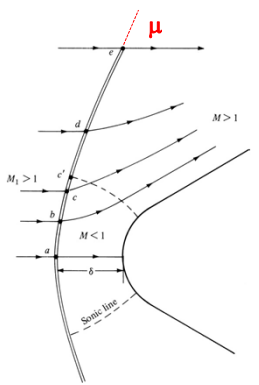
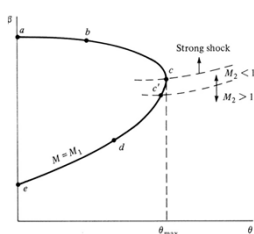


Figure illustrates the intersection of two left-running shocks generated at corners A and B . The intersection occurs at point C , at which the two shocks merge and propagate as the stronger shock CD , usually along with a weak reflected wave CE . **This reflected wave is necessary to adjust the flow so that the velocities in regions 4 and 5 are in the same direction.** Again, a slip line CF trails downstream of the intersection point.

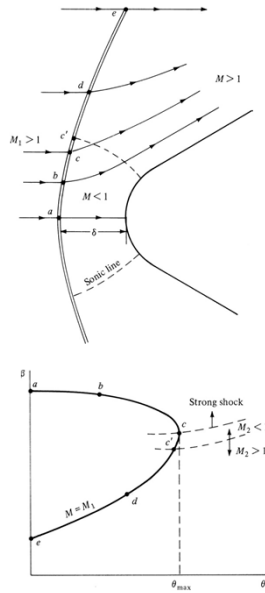
DETACHED SHOCK WAVE IN FRONT OF A BLUNT BODY



- The curved bow shock stands in front of a blunt body in a supersonic flow. Here, the shock wave stands a distance δ in front of the nose of the blunt body; δ is defined as the **shock detachment distance**.
- At point a , the shock wave is **normal shock wave**. Away from point a , the shock wave gradually becomes curved and weaker, eventually evolving into a Mach wave at large distances from the body (illustrated by point e in Fig.).
- Consider the $\theta\beta M$ diagram in conjunction with Fig. In Fig, **point a corresponds to the normal shock**, and **point e corresponds to the Mach wave**.
- Slightly above the centerline, **at point b , the shock is oblique but pertains to the strong shock-wave solution in $\theta\beta M$ diagram**. The flow is deflected slightly upward behind the shock at point b .



DETACHED SHOCK WAVE IN FRONT OF A BLUNT BODY



- As we move further along the shock from *b*, the wave angle becomes more oblique, and the flow deflection increases until we encounter point *c*. **Point *c* on the bow shock corresponds to the maximum deflection angle shown in $\theta\beta M$ diagram.**
- Above point *c*, from *c* to *e*, all points on the shock correspond to the weak shock solution.**
- Slightly above point *c*, at point *c'*, the flow behind the shock becomes sonic.
- From *a* to *c'*, the flow is subsonic behind the bow shock; from *c'* to *e*, it is supersonic behind the bow shock.**
- Hence, the flow field between the curved bow shock and the blunt body is a mixed region of both subsonic and supersonic flow. The dividing line between the subsonic and supersonic regions is called the **sonic line**, shown as the dashed.

EXAMPLE 9.8

Consider the detached curved bow shock wave in front of the two-dimensional parabolic blunt body drawn in Figure 9.25. The freestream is at Mach 8. Consider the two streamlines passing through the shock at points *a* and *b* shown in Figure 9.25. The wave angle at point *a* is 90° , and that at point *b* is 60° . Calculate and compare the value of entropy (relative to the free stream) for streamlines *a* and *b* in the flow behind the shock.

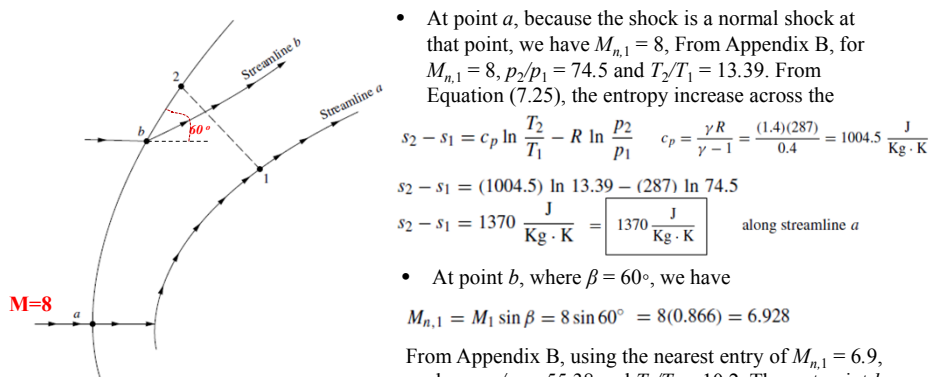


Figure 9.25 Two streamlines crossing a detached bow shockwave in front of a blunt body at Mach 8.

The entropy along streamline *b* is smaller than that along streamline *a* because streamline *b* passes through a weaker part of the bow shock wave.

- At point *a*, because the shock is a normal shock at that point, we have $M_{n,1} = 8$. From Appendix B, for $M_{n,1} = 8$, $p_2/p_1 = 74.5$ and $T_2/T_1 = 13.39$. From Equation (7.25), the entropy increase across the

$$s_2 - s_1 = c_p \ln \frac{T_2}{T_1} - R \ln \frac{p_2}{p_1} \quad c_p = \frac{\gamma R}{\gamma - 1} = \frac{(1.4)(287)}{0.4} = 1004.5 \frac{\text{J}}{\text{Kg} \cdot \text{K}}$$

$$s_2 - s_1 = (1004.5) \ln 13.39 - (287) \ln 74.5$$

$$s_2 - s_1 = 1370 \frac{\text{J}}{\text{Kg} \cdot \text{K}} = \boxed{1370 \frac{\text{J}}{\text{Kg} \cdot \text{K}}} \quad \text{along streamline } a$$

- At point *b*, where $\beta = 60^\circ$, we have

$$M_{n,1} = M_1 \sin \beta = 8 \sin 60^\circ = 8(0.866) = 6.928$$

From Appendix B, using the nearest entry of $M_{n,1} = 6.9$, we have $p_2/p_1 = 55.38$ and $T_2/T_1 = 10.2$. Thus, at point *b*,

$$s_2 - s_1 = c_p \ln \frac{T_2}{T_1} - R \ln \frac{p_2}{p_1} = (1004.5) \ln 10.2 - (287) \ln 55.38$$

$$s_2 - s_1 = \boxed{1180 \frac{\text{J}}{\text{Kg} \cdot \text{K}}} \quad \text{along streamline } b$$

Crocco's theorem

A combination of the momentum equation and the combined first and second laws of thermodynamics:

$$T \nabla s = \nabla h_o - \mathbf{V} \times (\nabla \times \mathbf{V})$$

Where ∇s is the entropy gradient, ∇h_o is the gradient in the total enthalpy, and $\nabla \times \mathbf{V}$ is the vorticity.

Crocco's theorem is presented simply to emphasize an **important feature of the flow behind the curved shock**. The flow is adiabatic, hence ∇h_o is zero everywhere in the flow. However, ∇s is finite, and therefore from Crocco's theorem **$\nabla \times \mathbf{V}$ must be finite**.

Conclusion:

- The flow field behind a **curved shock wave** is **rotational**.
- As a result, a **velocity potential with all its analytical advantages discussed earlier in this book can not be defined for the blunt-body flow field**.
- Consequently, the flow field behind a curved shock is computed by means of CFD numerical solutions of the continuity, momentum, and energy equations. Such computational fluid dynamic solutions are discussed in Section 13.5.

PRANDTL-MEYER EXPANSION WAVES

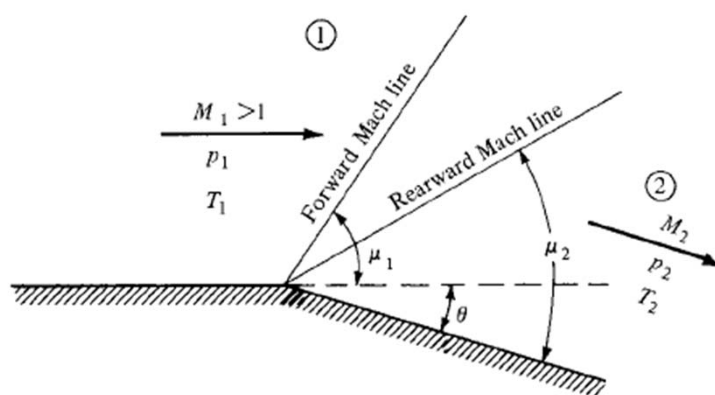
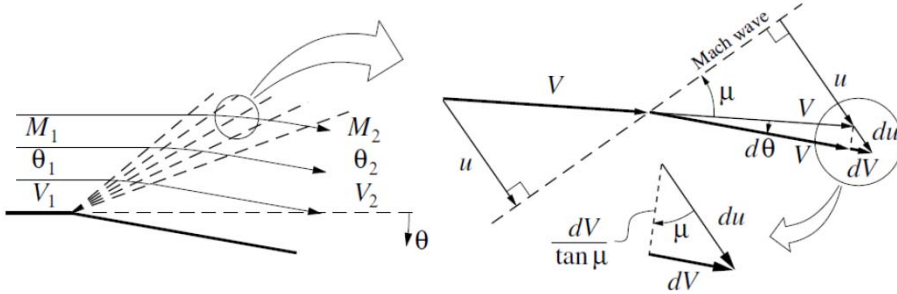


Figure 9.26 Prandtl-Meyer expansion.

Prandtl-Meyer Waves

An expansion fan, sometimes also called a **Prandtl-Meyer expansion wave**, **can be considered as a continuous sequence of infinitesimal Mach expansion waves**. To analyze this continuous change, we will now consider the flow angle θ to be a flow field variable, like M or V .

Across each Mach wave of the fan, the flow direction changes by $d\theta$, while the speed changes by dV . Oblique-shock analysis dictates that only the normal velocity component u can change across any wave, so that dV must be entirely due to the normal-velocity change du .



From the u - V and du - dV velocity triangles, it is evident that $d\theta$ and dV are related by

$$d\theta = \frac{dV}{\tan \mu} \frac{1}{V}$$

assuming $d\theta$ is a small angle.

With $\sin \mu = 1/M$, we have

$$\frac{1}{\tan \mu} = \frac{\cos \mu}{\sin \mu} = \frac{\sqrt{1 - \sin^2 \mu}}{\sin \mu} = \frac{\sqrt{1 - 1/M^2}}{1/M} = \sqrt{M^2 - 1}$$

and so the flow relation above becomes

$$d\theta = \sqrt{M^2 - 1} \frac{dV}{V} \quad (1)$$

This is a differential equation which relates a change $d\theta$ in the flow angle to a change dV in the flow speed throughout the expansion fan.

Prandtl-Meyer Function

The differential equation (1) can be integrated if we first express V in terms of M.

$$\begin{aligned} V &= Ma = Ma_o \left(1 + \frac{\gamma-1}{2}M^2\right)^{-1/2} \\ \ln V &= \ln M + \ln a_o - \frac{1}{2} \ln \left(1 + \frac{\gamma-1}{2}M^2\right) \\ \frac{dV}{V} &= \frac{dM}{M} - \frac{1}{2} \left(1 + \frac{\gamma-1}{2}M^2\right)^{-1} \frac{\gamma-1}{2} 2M dM \\ \frac{dV}{V} &= \frac{1}{1 + \frac{\gamma-1}{2}M^2} \frac{dM}{M} \quad d\theta = \sqrt{M^2 - 1} \frac{dV}{V} \end{aligned} \quad (1)$$

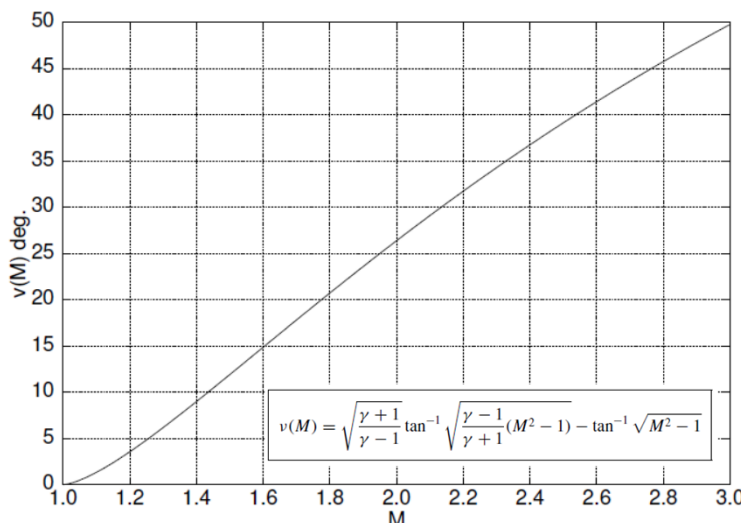
Equation (1) then becomes $d\theta = \frac{\sqrt{M^2 - 1}}{1 + \frac{\gamma-1}{2}M^2} \frac{dM}{M}$

which can now be integrated from any point 1 to any point 2 in the Prandtl-Meyer wave.

$$\int_{\theta_1}^{\theta_2} d\theta = \int_{M_1}^{M_2} \frac{\sqrt{M^2 - 1}}{1 + \frac{\gamma-1}{2}M^2} \frac{dM}{M} \quad (2) \quad \rightarrow \quad \theta_2 - \theta_1 = \nu(M_2) - \nu(M_1) \quad (3)$$

$$\nu(M) = \sqrt{\frac{\gamma+1}{\gamma-1}} \tan^{-1} \sqrt{\frac{\gamma-1}{\gamma+1}(M^2 - 1)} - \tan^{-1} \sqrt{M^2 - 1} \quad (4)$$

Prandtl-Meyer Function $\nu(M)$

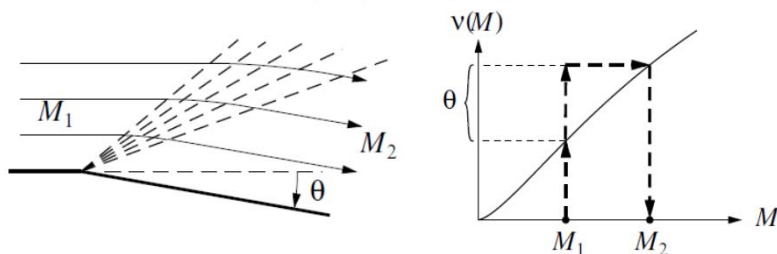


It is tabulated as a function of M in Appendix C.

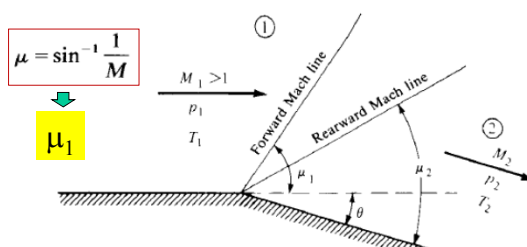
$$\theta_2 - \theta_1 = \nu(M_2) - \nu(M_1) \quad (3)$$

Equation (3) can be applied to any two points within an expansion fan, but the most common use is to relate the **two flow conditions before and after the fan**. Reverting back to our previous notation where θ is the total turning of the corner, the relation between θ and the upstream and downstream Mach number is

$$\theta = \nu(M_2) - \nu(M_1) \quad (5)$$



This can be considered an implicit definition of $M_2(M_1, \theta)$, which can be evaluated graphically using the $\theta(M)$ function plot, as shown in the figure.



Prandtl Meyer Expansion Waves Analysis: Summary

- For the given M_1 , obtain $\nu(M_1)$ from App. C.

$$\nu(M) \equiv \sqrt{\frac{\gamma+1}{\gamma-1}} \arctan \sqrt{\frac{\gamma-1}{\gamma+1} (M^2 - 1)} - \arctan \sqrt{M^2 - 1}$$

- Calculate $\nu(M_2)$ from Eq. (9.43), using the known θ and the value of $\nu(M_1)$ obtained in step 1.

$$\theta = \nu(M_2) - \nu(M_1) \rightarrow \nu(M_2)$$

- Obtain M_2 from App. C corresponding to the value of $\nu(M_2)$ from step 2.

- The expansion wave is isentropic; hence, p_0 and T_0 are constant through the wave. That is, $T_{0,2} = T_{0,1}$ and $p_{0,2} = p_{0,1}$. From Eq. (8.40), we have

$$\frac{T_2}{T_1} = \frac{T_2/T_{0,2}}{T_1/T_{0,1}} = \frac{1 + [(\gamma-1)/2]M_1^2}{1 + [(\gamma-1)/2]M_2^2} \rightarrow T_2 \quad (9.44)$$

$$\mu = \sin^{-1} \frac{1}{M}$$

$$\mu_2$$

From Eq. (8.42), we have

$$\frac{p_2}{p_1} = \frac{p_2/p_0}{p_1/p_0} = \left(\frac{1 + [(\gamma-1)/2]M_1^2}{1 + [(\gamma-1)/2]M_2^2} \right)^{\gamma/(\gamma-1)} \rightarrow P_2 \quad (9.45)$$

Since we know both M_1 and M_2 , as well as T_1 and p_1 , Eqs. (9.44) and (9.45) allow the calculation of T_2 and p_2 downstream of the expansion wave.

Example 9.7. A supersonic flow with $M_1 = 1.5$, $p_1 = 1 \text{ atm}$, and $T_1 = 288 \text{ K}$ is expanded around a sharp corner (see Fig. 9.23) through a deflection angle of 15° . Calculate M_2 , p_2 , T_2 , $p_{0,2}$, $T_{0,2}$, and the angles that the forward and rearward Mach lines make with respect to the upstream flow direction.

Solution. From App. C, for $M_1 = 1.5$, $\nu_1 = 11.91^\circ$. From Eq. (9.43), $\nu_2 = \nu_1 + \theta = 11.91 + 15 = 26.91^\circ$. Thus, $M_2 = 2.0$ (rounding to the nearest entry in the table).

From App. A, for $M_1 = 1.5$, $p_{0,1}/p_1 = 3.671$ and $T_{0,1}/T_1 = 1.45$, and for $M_2 = 2.0$, $p_{0,2}/p_2 = 7.824$ and $T_{0,2}/T_2 = 1.8$.

Since the flow is isentropic, $T_{0,2} = T_{0,1}$ and $p_{0,2} = p_{0,1}$. Thus,

$$p_2 = \frac{p_2}{p_{0,2}} \frac{p_{0,2}}{p_{0,1}} p_1 = \frac{1}{7.824} (1)(3.671)(1 \text{ atm}) = 0.469 \text{ atm}$$

$$T_2 = \frac{T_2}{T_{0,2}} \frac{T_{0,2}}{T_{0,1}} T_1 = \frac{1}{1.8} (1)(1.45)(288) = 232 \text{ K}$$

$$p_{0,2} = p_{0,1} = \frac{p_{0,1}}{p_1} p_1 = 3.671(1 \text{ atm}) = 3.671 \text{ atm}$$

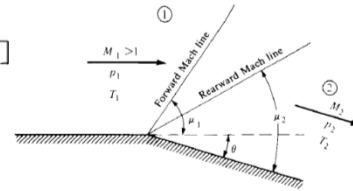
$$T_{0,2} = T_{0,1} = \frac{T_{0,1}}{T_1} T_1 = 1.45(288) = 417.6 \text{ K}$$

Returning to Fig. 9.23, we have

$$\text{Angle of forward Mach line} = \mu_1 = 41.81^\circ$$

$$\mu = \arcsin(1/M)$$

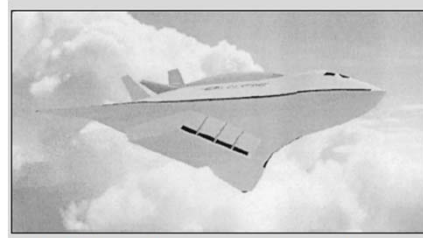
$$\text{Angle of rearward Mach line} = \mu_2 - \theta = 30 - 15 = 15^\circ$$



(a) SCRAMjet-powered air-to-surface-missile concept



(b) SCRAMjet-powered strike/reconnaissance vehicle concept



(c) SCRAMjet-powered space access vehicle concept

SCRAMjet Engine Inlet Design for Mach 8–12 Hypersonic Aircraft

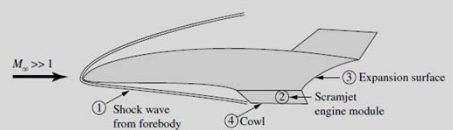


Figure 9.30 Sketch of a generic hypersonic vehicle powered by a SCRAMjet engine.

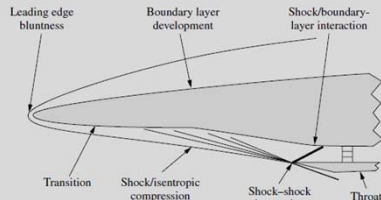


Figure 9.31 Sketch of some of the flow features on the forebody of a SCRAMjet-powered hypersonic vehicle.

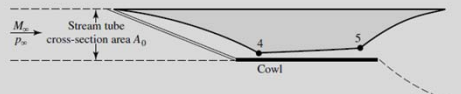


Figure 9.32 Flow path through a SCRAMjet engine.

The side view of a generic hypersonic vehicle powered by a SCRAMjet is shown in [Figure 9.30](#). Essentially, the entire bottom surface of the vehicle is an integrated portion of the air-breathing SCRAMjet engine.

The forebody shock wave (1) from the nose of the vehicle is the initial part of the **compression** process for the engine. Air flowing through this shock wave is compressed, and then enters the SCRAMjet engine module (2) where it is further compressed by reflected shock waves inside the engine duct, mixed with fuel, and then expanded out the back end of the module. The back end of the vehicle is scooped out (3) in order to further enhance the expansion of the exhaust gas. At the design flight condition, **the forebody shock wave impinges right at the leading edge of the cowl** (4), so that all the flow passing through the shock will enter the engine, rather than some of the air spilling around the external surface.

SCRAMjet Engine Inlet Design for Mach 8–12 Hypersonic Aircraft

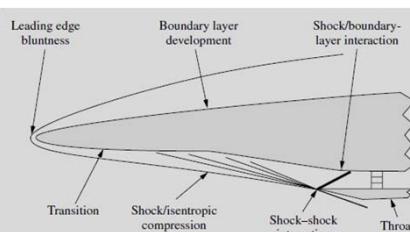


Figure 9.31 Sketch of some of the flow features on the forebody of a SCRAMjet-powered hypersonic vehicle.

It is also possible to further compress the air before it enters the engine module by creating an **isentropic compression wave** downstream of the shock, as shown in Figure 9.31. Here, the bottom surface of the body creates drag and aerodynamic heating, and when a shock wave impinges on the form an isentropic compression wave that will boundary layer, flow separation and local focus at the leading edge of the cowl, right where reattachment may occur, creating local regions of the forebody shock wave is impinging as well. An isentropic compression wave is the opposite of the interaction problem). There is always the important isentropic expansion wave discussed in Section 9.6, question as to where transition from laminar to turbulent boundary layer flow occurs along the same Prandtl-Meyer function, except in this body, because turbulent boundary layers result in increased aerodynamic heating and skin.

wave, and the pressure increases. To create such an isentropic compression wave in reality is quite difficult; the contour of the body surface must be a specific shape for a specific upstream Mach number, and most efforts over the years to produce isentropic compression waves in various supersonic and hypersonic flow devices have usually resulted in the wave prematurely coalescing into several weak shock waves with associated entropy increases and total pressure loss. Other physical phenomena that influence SCRAMjet engine performance and vehicle aerodynamics are also noted in Figure 9.31. The leading edge must be blunted in order to reduce the aerodynamic heating at the nose. The viscous boundary layer over the shock, as shown in Figure 9.31. Here, the bottom surface of the body creates drag and aerodynamic heating, and when a shock wave impinges on the form an isentropic compression wave that will boundary layer, flow separation and local focus at the leading edge of the cowl, right where reattachment may occur, creating local regions of the forebody shock wave is impinging as well. An isentropic compression wave is the opposite of the interaction problem). There is always the important isentropic expansion wave discussed in Section 9.6, question as to where transition from laminar to turbulent boundary layer flow occurs along the same Prandtl-Meyer function, except in this body, because turbulent boundary layers result in increased aerodynamic heating and skin.

EXAMPLE 9.10

In the preceding discussion on SCRAMjet engines, an isentropic compression wave was mentioned as one of the possible compression mechanisms. Consider the isentropic compression surface sketched in Figure 9.35a. The Mach number and pressure upstream of the wave are $M_1 = 10$ and $p_1 = 1 \text{ atm}$, respectively. The flow is turned through a total angle of 15° . Calculate the Mach number and pressure in region 2 behind the compression wave.

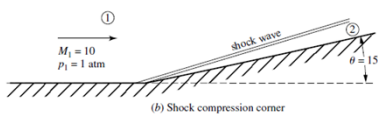
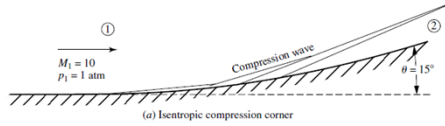


Figure 9.35 Figures for (a) Example 9.9 and (b) Example 9.10.

Solution

From Appendix C, for $M_1 = 10$, $v_1 = 102.3^\circ$. In Region 2,

$$v_2 = v_1 - \theta = 102.3 - 15 = 87.3^\circ$$

From Appendix C for $v_2 = 87.3^\circ$, we have (closest entry)

$$M_2 = 6.4$$

From Appendix A, for $M_1 = 10$, $p_{0,1}/p_1 = 0.4244 \times 10^5$ and for $M_2 = 6.4$, $p_{0,2}/p_2 = 0.2355 \times 10^4$. Since the flow is isentropic, $p_{0,2} = p_{0,1}$, and hence

$$\begin{aligned} p_2 &= \left(\frac{p_2}{p_{0,2}} \right) \left(\frac{p_{0,2}}{p_{0,1}} \right) \left(\frac{p_{0,1}}{p_1} \right) p_1 = \left(\frac{1}{0.2355 \times 10^4} \right) (1)(0.4244 \times 10^5)(1) \\ &= 18.02 \text{ atm} \end{aligned}$$

EXAMPLE 9.11

Consider the flow over a compression corner with the same upstream conditions of $M_1 = 10$ and $p_1 = 1 \text{ atm}$ as in Example 9.10, and the same turning angle of 15° , except in this case the corner is sharp and the compression takes place through an oblique shock wave as sketched in Figure 9.35b. Calculate the downstream Mach number, static pressure, and total pressure in region 2. Compare the results with those obtained in Example 9.10, and comment on the significance of the comparison.

Solution

From Figure 9.9 for $M_1 = 10$ and $\theta = 15^\circ$, the wave angle is $\beta = 20^\circ$. The component of the upstream Mach number perpendicular to the wave is

$$M_{n,1} = M_1 \sin \beta = (10) \sin 20^\circ = 34.2$$

From Appendix B for $M_{n,1} = 3.42$, we have (nearest entry), $p_2/p_1 = 13.32$, $p_{0,2}/p_{0,1} = 0.2322$, and $M_{n,2} = 0.4552$. Hence

$$\begin{aligned} M_2 &= \frac{M_{n,2}}{\sin(\beta - \theta)} = \frac{0.4552}{\sin(20 - 15)} = 5.22 \\ p_2 &= (p_2/p_1)p_1 = 13.32(1) = 13.32 \text{ atm} \end{aligned}$$

The total pressure in region 1 can be obtained from Appendix A as follows. For $M_1 = 10$, $p_{0,1}/p_1 = 0.4244 \times 10^5$. Hence, the total pressure in region 2 is

$$p_{0,2} = \left(\frac{p_{0,2}}{p_{0,1}} \right) (p_1) = (0.2322)(0.4244 \times 10^5)(1) = 9.85 \times 10^3 \text{ atm}$$

As a check, we can calculate $p_{0,2}$ as follows. (This check also alerts us to the error incurred when we round to the nearest entry in the tables.) From Appendix A for $M_2 = 5.22$, $p_{0,2}/p_2 = 0.6661 \times 10^3$ (nearest entry). Hence,

$$p_{0,2} = \left(\frac{p_{0,2}}{p_2} \right) (p_2) = (0.6661 \times 10^3)(13.32) = 8.87 \times 10^3 \text{ atm}$$

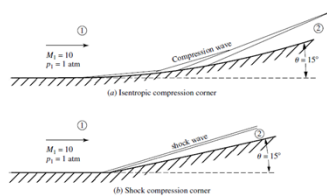
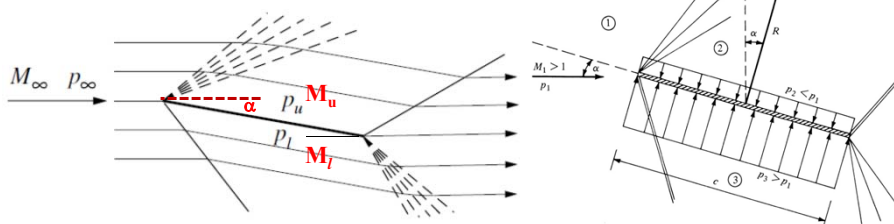


Figure 9.35 Figures for (a) Example 9.9 and (b) Example 9.10.

Shock-Expansion Theory

The combination of **oblique-shock relations** and **Prandtl-Meyer wave relations** constitutes **Shock-Expansion Theory**, which can be used to determine the flow properties and forces about simple 2-D shapes in supersonic flow.

Flat-plate supersonic airfoil

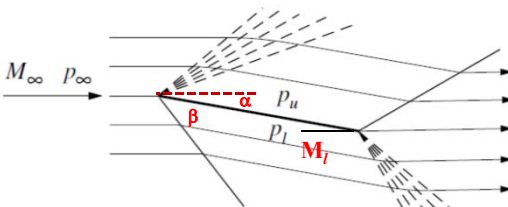


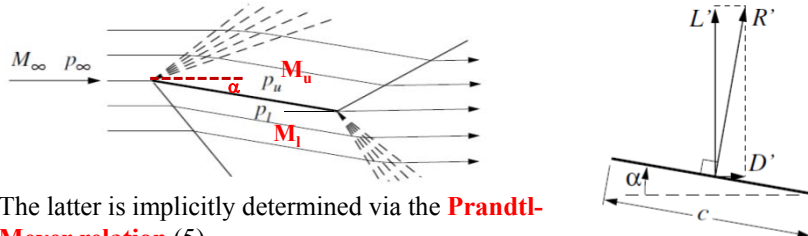
A flat plate is the simplest supersonic airfoil. When set at an **angle of attack α** , the leading edge point effectively is a convex corner to the upper surface flow, with turning angle $\theta=\alpha$. The upper flow then passes through the resulting **Prandtl-Meyer expansion**, which increases its Mach number from $M_1 = M_\infty$, to a larger value $M_2 = M_u$. The lower flow then passes through the **oblique-shock**, which decreases its Mach number from $M_1 = M_\infty$, to a smaller value $M_2 = M_l$.

Oblique-Shock Analysis: Summary

Starting from the known upstream Mach number M_1 and the flow deflection angle (body surface angle) θ , the oblique-shock analysis proceeds as follows.

$$\begin{aligned} \tan \theta &= \frac{2}{\tan \beta} \frac{M_1^2 \sin^2 \beta - 1}{M_1^2 (\gamma + \cos 2\beta) + 2} & M_{n2}^2 &= \frac{1 + \frac{\gamma-1}{2} M_{n1}^2}{\gamma M_{n1}^2 - \frac{\gamma-1}{2}} & M_2 &= \frac{M_{n2}}{\sin(\beta - \theta)} \\ \theta, M_1 &\xrightarrow{\text{Eq.(13)}} \beta & M_{n1} &\xrightarrow{\text{Eq.(6)}} M_{n1} & M_{n2}, M_2, \frac{p_2}{p_1}, \frac{p_2}{p_1}, \frac{h_2}{h_1}, \frac{p_{o2}}{p_{o1}} & \\ \theta = \alpha & \\ M_1 = M_\infty & \quad M_{n1} = M_1 \sin \beta & & & \frac{p_2}{p_1} &= 1 + \frac{2\gamma}{\gamma+1} (M_{n1}^2 - 1) \\ & & & & P_1 = P_\infty & \\ & & & & P_2 = P_l & \end{aligned}$$





The latter is implicitly determined via the **Prandtl-Meyer relation** (5).

$$\alpha = \nu(M_u) - \nu(M_\infty) \rightarrow M_u(M_\infty, \alpha)$$

The corresponding upper-surface pressure is then given by the isentropic relation.

$$p_u = p_\infty \left(\frac{1 + \frac{\gamma-1}{2} M_\infty^2}{1 + \frac{\gamma-1}{2} M_u^2} \right)^{\gamma/(\gamma-1)}$$

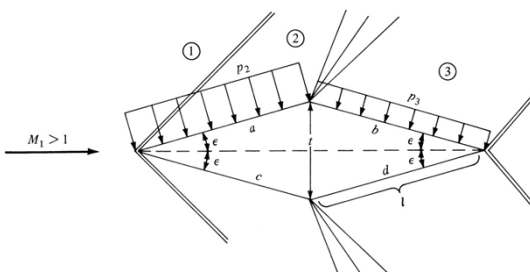
The pressure difference produces a resultant force/span R' acting normal to the plate, which can be resolved into lift and drag components.

$$R' = (p_e - p_u) c \quad L' = (p_e - p_u) c \cos \alpha \quad D' = (p_e - p_u) c \sin \alpha$$

It's worthwhile to note that this supersonic airfoil has a **nonzero drag** even if the flow is being assumed inviscid. The drag D is associated with the viscous dissipation occurring in the oblique shock waves, and hence is called **wave drag**. This wave drag is an additional drag component in supersonic flow, and must be added to the usual viscous friction drag, and also the induced drag in 3-D cases.

Diamond-Shape Airfoil

- Assume the airfoil is at 0° angle of attack.
- The supersonic flow over the airfoil is first compressed and deflected through the **angle ϵ** by the oblique shock wave at the leading edge.
- At mid-chord, the flow is expanded through an **angle 2ϵ** , creating an expansion wave. At the trailing edge, the flow is turned back to the freestream direction through another oblique shock.
- The pressure distributions on the front and back faces of the airfoil are sketched in Fig; note that the pressures on **faces a and c** are uniform and equal to P_2 and that the pressures on **faces b and d** are also uniform but equal to P_3 , where $P_3 < P_2$.
- In the lift direction, perpendicular to the freestream, the pressure distributions on the top and bottom faces exactly cancel; i.e., $L' = 0$.

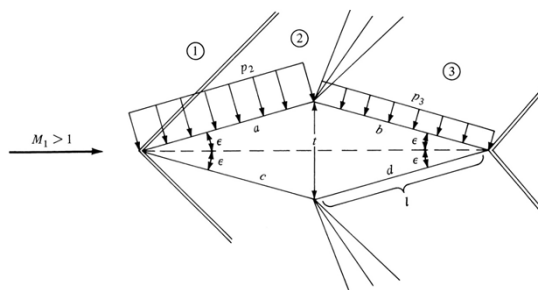


- In the drag direction, parallel to the freestream, **the pressure on the front faces *a* and *c* is larger than on the back faces *b* and *d***, and this results in a finite drag. To calculate this drag (per unit span), consider the geometry of the diamond airfoil in Fig, where l is the length of each face and t is the airfoil thickness. Then,

$$D' = 2(p_2 l \sin \epsilon - p_3 l \sin \epsilon) = 2(p_2 - p_3) \frac{t}{2}$$

$$D' = (p_2 - p_3)t$$

where P_2 is calculated from oblique shock theory, and P_3 is obtained from expansion-wave theory.



Example 9.8. Calculate the lift and drag coefficients for a flat plate at a 5° angle of attack in a Mach 3 flow.

Solution. Refer to Fig. 9.26. First, calculate p_2/p_1 on the upper surface. From Eq. (9.43),

$$\nu_2 = \nu_1 + \theta$$

where $\theta = \alpha$. From App. C, for $M_1 = 3$, $\nu_1 = 49.76^\circ$. Thus,

$$\nu_2 = 49.76^\circ + 5^\circ = 54.76^\circ$$

From App. C,

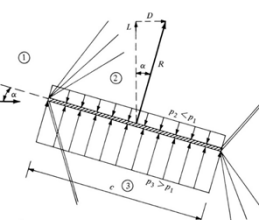
$$M_2 = 3.27$$

From App. A, for $M_1 = 3$, $p_{01}/p_1 = 36.73$; for $M_2 = 3.27$, $p_{02}/p_2 = 55$.

Since $p_{01} = p_{02}$,

$$\frac{p_2}{p_1} = \frac{p_{01}}{p_1} / \frac{p_{02}}{p_2} = \frac{36.73}{55} = 0.668$$

Next, calculate p_3/p_1 on the bottom surface. From the $\theta-\beta-M$ diagram (Fig. 9.7),

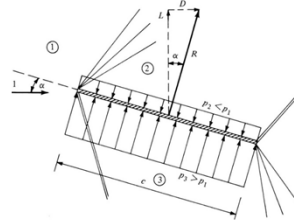


for $M_1 = 3$ and $\theta = 5^\circ$, $\beta = 23.1^\circ$. Hence,

$$M_{n,1} = M_1 \sin \beta = 3 \sin 23.1^\circ = 1.177$$

From App. B, for $M_{n,1} = 1.177$, $p_3/p_1 = 1.458$ (nearest entry).
Returning to Eq. (9.47), we have

$$L' = (p_3 - p_2)c \cos \alpha$$



The lift coefficient is obtained from

$$\begin{aligned} c_l &= \frac{L'}{q_1 S} = \frac{L'}{(\gamma/2)p_1 M_1^2 c} = \frac{2}{\gamma M_1^2} \left(\frac{p_3}{p_1} - \frac{p_2}{p_1} \right) \cos \alpha \\ &= \frac{2}{(1.4)(3)^2} (1.458 - 0.668) \cos 5^\circ = [0.125] \end{aligned}$$

From Eq. (9.48),

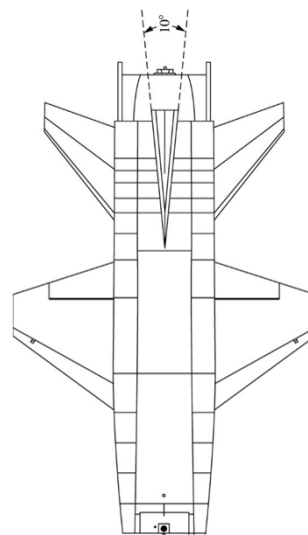
$$D' = (p_3 - p_2)c \sin \alpha \quad \frac{c_d}{c_l} = \tan \alpha$$

Hence,

$$c_d = c_l \tan \alpha = 0.125 \tan 5^\circ = 0.011$$

$$\begin{aligned} c_d &= \frac{D'}{q_1 S} = \frac{2}{\gamma M_1^2} \left(\frac{p_3}{p_1} - \frac{p_2}{p_1} \right) \sin \alpha \\ &= \frac{2}{(1.4)(3)^2} (1.458 - 0.668) \sin 5^\circ = [0.011] \end{aligned}$$

THE X-15 AND ITS WEDGE TAIL



EXAMPLE 9.13

Consider the flat plate shown in Figure 9.39a and the 10° included angle wedge shown in Figure 9.39b, both at an angle of attack of 10° in a Mach 7 airstream. (a) Calculate the lift coefficient of the flat plate. (b) Calculate the lift coefficient of the wedge.

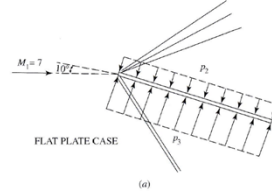
■ Solution

(a) First, consider the expansion wave over the top of the plate. From Appendix C, for $M_1 = 7$, $\nu_1 = 90.97^\circ$. From Equation (9.43)

$$\nu_2 = \nu_1 + \alpha = 90.97^\circ + 10^\circ = 100.97^\circ$$

Interpolating to obtain M_2 from Appendix C,

$$M_2 = 9 + \frac{100.97 - 99.32}{102.3 - 99.32} (1) = 9.56$$



Going to the isentropic flow tables in Appendix A, and interpolating for p_o/p between entries, we have $p_{o2}/p_2 = 0.33 \times 10^5$. Also from Appendix A, for $M_1 = 7$, we have $p_{o1}/p_1 = 0.14 \times 10^4$. Since p_o is constant across the expansion wave, then

$$\frac{p_2}{p_1} = \frac{p_{o1}/p_1}{p_{o2}/p_2} = \frac{0.414 \times 10^4}{0.33 \times 10^5} = 0.1255$$

Now consider the shock under the bottom of the plate in Figure 9.39a. From the $\theta-\beta-M$ diagram in Figure 9.9, for $M_1 = 7$ and $\alpha = 10^\circ$, $\beta = 16.5^\circ$,

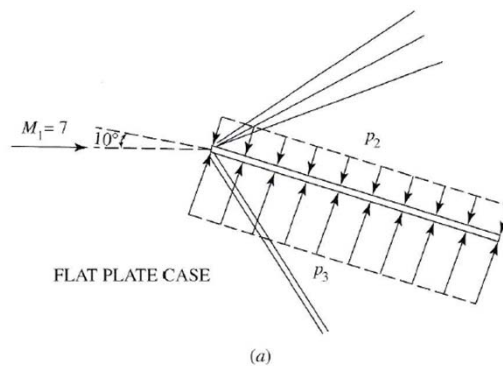
$$M_{n,1} = M_1 \sin \beta = 7 \sin 16.5^\circ = 1.99$$

From Appendix B, for $M_{n,1} = 1.99$, interpolating, we have

$$\frac{p_3}{p_1} = 4.407 + (0.093)(0.5) = 4.45$$

The lift coefficient for a supersonic or hypersonic flat plate was derived in Example 9.12 as

$$\begin{aligned} c_L &= \frac{2}{\gamma M_1^2} \left(\frac{p_3}{p_1} - \frac{p_2}{p_1} \right) \cos \alpha \\ &= \frac{2}{(1.4)(7)^2} (4.45 - 0.1255) = \boxed{0.126} \end{aligned}$$



(b) First consider the expansion wave over the top of the wedge.

$$v_2 = v_1 + 5^\circ = 90.97^\circ + 5^\circ = 95.97^\circ$$

From Appendix C, interpolating,

$$M_2 = 8 + \frac{95.97 - 96.62}{99.32 - 95.62} (1) = 8.1$$

From Appendix A, interpolating,

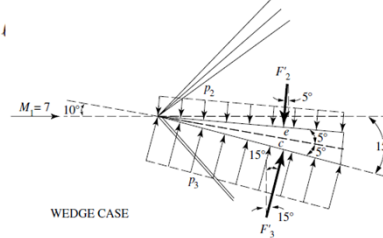
$$\frac{p_{o2}}{p_2} = 0.9763 \times 10^4 + (0.211 \times 10^5 - 0.9763 \times 10^4)(1) = 1.0897 \times 10^4$$

The relation between the chord length, c and the length of the face of the wedge ℓ is

$$\ell = \frac{c}{\cos 5^\circ} = \frac{c}{0.996} = 1.004c$$

The force per unit span, F'_2 , acting on the top surface of the wedge, is

$$F'_2 = p_2 \ell = \left(\frac{p_{o1}/p_1}{p_{o2}/p_2} \right) p_1 \ell$$



For $M_1 = 7$, from Appendix A, $p_{o1}/p_1 = 0.414 \times 10^4$. Thus,

$$F'_2 = \left(\frac{0.414 \times 10^4}{1.0897 \times 10^4} \right) p_1 \ell = 0.38 p_1 \ell$$

Considering the shock wave under the bottom of the wedge, we have, from the $\theta-\beta-M$ diagram, for $M_1 = 7$ and $\theta = 15^\circ$, $\beta = 23.5^\circ$. Thus,

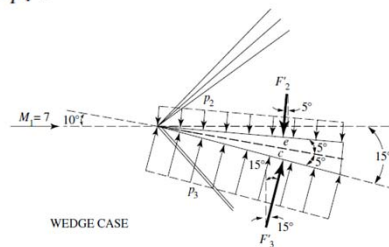
$$M_{n,1} = M_1 \sin \beta = 7 \sin 23.5^\circ = 2.79$$

From Appendix B, interpolating,

$$\frac{p_3}{p_1} = 8.656 + (8.98 - 8.656)(0.8) = 8.915$$

Thus, the force per unit span, F'_3 , acting on the bottom surface of the wedge, is

$$F'_3 = p_3 \ell = \left(\frac{p_3}{p_1} \right) p_1 \ell = 8.915 p_1 \ell$$



The lift per unit span is the combination of the *components* of F'_2 and F'_3 perpendicular to the free stream. Examining Figure 9.39b, we see that

$$L' = F'_3 \cos 15^\circ - F'_2 \cos 5^\circ = 0.9659F'_3 - 0.9962F'_2$$

$$L' = (0.9659)(8.915)p_1 \ell - (0.9962)(0.38)p_1 \ell$$

$$L' = 8.232p_1 \ell$$

However, $\ell = 1.004c$, Thus,

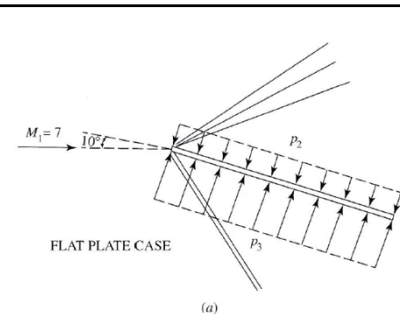
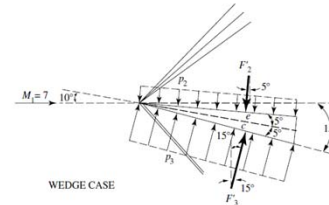
$$L' = 8.232p_1(1.004c) = 8.265p_1c$$

The lift coefficient is

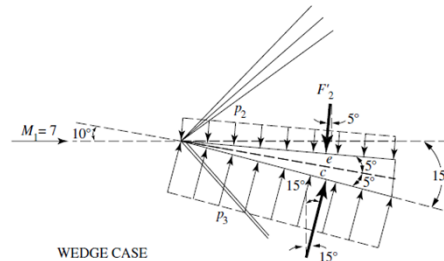
$$c_\ell = \frac{L'}{q_1 c} = \frac{L'}{(\gamma/2)p_1 M_1^2 c} = \frac{2L'}{\gamma p_1 M_1^2 c}$$

Since $L' = 8.265p_1c$, we have

$$c_\ell = \frac{2(8.265)p_1c}{(1.4)p_1(7)^2c} = \boxed{0.241}$$



$$c_\ell = \boxed{0.126}$$



$$c_\ell = \boxed{0.241}$$

VISCOUS FLOW: SHOCK-WAVE/ BOUNDARY-LAYER INTERACTION

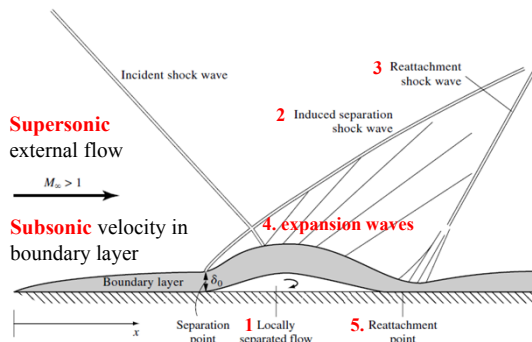


Figure 9.40 Schematic of the shock-wave/boundary-layer interaction.

1. The large pressure rise across the shock wave acts as a **severe adverse pressure gradient** imposed on the boundary layer, thus causing the boundary layer to locally **separate** from the surface.
2. In turn, the separated boundary layer deflects the external supersonic flow into itself, thus inducing a second shock wave, identified here as the **induced separation shock wave**.
3. The separated boundary layer subsequently turns back toward the plate, **reattaching** to the surface at some downstream location. the supersonic flow is deflected into itself, causing a third shock wave called the **reattachment shock**.
4. Between the separation and reattachment shocks, where the boundary layer is turning back toward the surface, the supersonic flow is turned away from itself, generating **expansion waves**.